Parkinsonism and Related Disorders xxx (2016) 1–7

Contents lists available at ScienceDirect

Parkinsonism and Related Disorders

journal homepage: www.elsevier.com/locate/parkreldis

Comparison of transcranial sonography-magnetic resonance fusion imaging in Wilson's and early-onset Parkinson's diseases

Jana Mašková [a], David Školoudík [a, b], Andrea Burgetová [c], Ondřej Fiala [a, d], Radan Brůha [e], Daniela Záhoráková [f], Tereza Serranová [a], Matěj Slovák [a], Olga Ulmanová [a], Evžen Růžička [a], Petr Dušek [a, g, *]

[a] Department of Neurology and Center of Clinical Neuroscience, Charles University in Prague, 1st Faculty of Medicine and General University Hospital in Prague, Kateřinská 30, 128 21, Prague, Czech Republic
[b] Department of Nursing, Faculty of Health Science, Palacky University Olomouc, Tř. Svobody 8, 771 11, Olomouc, Czech Republic
[c] Department of Radiology, Charles University in Prague, 1st Faculty of Medicine and General University Hospital in Prague, Kateřinská 30, 128 21, Prague, Czech Republic
[d] Institute of Neuropsychiatric Care (INEP), Křižíkova 264/22, 186 00, Prague, Czech Republic
[e] 4th Department of Internal Medicine, Charles University in Prague, 1st Faculty of Medicine and General University Hospital in Prague, U Nemocnice 2, 128 08, Prague, Czech Republic
[f] Department of Pediatrics and Adolescent Medicine, Charles University in Prague, 1st Faculty of Medicine and General University Hospital in Prague, Ke Karlovu 2, 121 00, Prague, Czech Republic
[g] Institute of Neuroradiology, Universitaetsmedizin Goettingen, Robert-Koch-Str. 40, 37075, Goettingen, Germany

ARTICLE INFO

Article history:
Received 9 October 2015
Received in revised form
20 April 2016
Accepted 26 April 2016

Keywords:
Transcranial sonography
MRI
Wilson's disease
Early-onset Parkinson's disease
Copper

ABSTRACT

Introduction: Wilson's disease (WD) is a hereditary disorder caused by *ATP7B* mutations resulting in systemic copper accumulation. WD may manifest as early-adulthood parkinsonism; and atypical cases may be difficult to distinguish from early-onset Parkinson's disease (EO-PD), a neurodegenerative disorder with onset ≤40 years of age. The aim of our study was to compare transcranial sonography (TCS) −magnetic resonance fusion imaging in WD and EO-PD and examine whether TCS can provide clinically useful information.

Methods: We examined 22 WD, 16 EO-PD, and 24 healthy control subjects. We measured echogenicity and determined presence of MRI signal changes in T2-weighted images in the substantia nigra (SN) and lentiform nucleus (NL). TCS with the capability of magnetic resonance fusion and Virtual Navigator was used. The echogenicity indices of SN and NL were processed using digital image analysis to eliminate subjective evaluation errors.

Results: Mean SN echogenicity index in EO-PD (39.8 ± 5.9 [SD]) was higher compared to WD (28.0 ± 4.6, $p < 0.0001$) and control subjects (28.8 ± 4.9, $p < 0.0001$). Mean NL echogenicity index was higher in WD (117.5 ± 37.0) compared to EO-PD (61.6 ± 5.4, $p < 0.0001$) and control subjects (54.9 ± 11.2, $p < 0.0001$). The SN hyperechogenicity had sensitivity 93.8%, and specificity 90.9%, while the NL hyperechogenicity had sensitivity 95.5% and specificity 93.8% for differentiation of WD and EO-PD. NL hyperechogenicity was more pronounced in WD subjects with putaminal MRI T2 hyperintensity ($p < 0.05$) but was also present in subjects without MRI abnormality.

Conclusions: There are distinct TCS findings in WD and EO-PD complementary to MRI that can be utilized as highly sensitive and specific biomarkers of these disorders.

1. Introduction

Wilson's disease (WD) is a hereditary disorder caused by *ATP7B* mutations resulting in copper accumulation in liver and brain. Timely diagnosis is essential since patients have a good prognosis if the treatment is provided in the early stage [1]. Diagnosis of

* Corresponding author. Dept. of Neurology and Center of Clinical Neuroscience, Charles University in Prague, 1st Faculty of Medicine and General University Hospital in Prague, Katerinska 30, 120 00, Praha 2, Czech Republic.
E-mail address: petr.dusek@vfn.cz (P. Dušek).

http://dx.doi.org/10.1016/j.parkreldis.2016.04.031
1353-8020/

neurological WD is straightforward in the majority of cases when typical biochemical abnormalities are present [2]. However, the diagnosis may be difficult in atypical cases that do not fulfill all the clinical and laboratory criteria [3]. Moreover, genetic confirmation may be difficult since *ATP7B* gene is large and more than 500 mutations were described [1], some of them with questionable pathogenicity [4].

According to guidelines, every patient with young adulthood-onset movement disorder should undergo screening for WD. WD may manifest with parkinsonism, either isolated or in combination with other symptoms such as dystonia, kinetic tremor or ataxia. In early-onset Parkinson's disease (EO-PD), parkinsonism is frequently accompanied by psychiatric symptoms and dystonia [5]. Therefore, the importance of the differential diagnosis between EO-PD and WD may arise, particularly in cases with atypical symptoms and/or inconclusive results of biochemical examinations.

Transcranial sonography (TCS) is a validated tool in the diagnosis of an early stage of PD [6] as well as in the differential diagnosis of PD and atypical parkinsonian syndromes [6,7] and dopa-responsive dystonia [8]. Typical findings in PD consist particularly of the hyperechogenicity and enlarged echogenic size of substantia nigra (SN) [6,9,10]. In the neurological form of WD, the echogenicity of SN is variable, while the hyperechogenicity of the lentiform nucleus (NL) has been consistent across studies [11–15]. It is unclear how echogenicity changes in WD interrelate to MRI abnormalities that typically consist of hyperintensity of basal ganglia, brainstem, and thalamus in T2-weighted (T2w) images [16].

Considering these different findings in EO-PD and WD patients, TCS could be a time-saving, low-cost, screening examination of these disorders. Potential drawbacks of TCS are limited anatomical clarity and dependence on examiner's subjective evaluation of hyperechogenicity. These obstacles are partially overcome by using Virtual Navigator for fusion of TCS and MRI which helps in precise identification of brain structures [17] and recently validated method of digital image analysis which reduces the sonographer's bias in the assessment of hyperechogenicity [18].

The aim of the study was to compare the echogenicity changes in SN and NL in EO-PD and WD in relation to MRI results and assess the utility of TCS as a screening examination in early-onset parkinsonism.

2. Methods

2.1. Patients

In WD patients, inclusion criterion was neurological WD with diagnosis established according to Leipzig criteria [19]. In EO-PD patients, inclusion criteria were diagnosis in accordance with the UK Parkinson's Disease Society Brain Bank criteria [20], and age at onset $\leq$ 40 years. For both groups, exclusion criteria were presence of deep brain stimulation (DBS) electrodes and insufficient temporal bone window for TCS examination. Out of 37 neurological WD patients from our database, 15 were not reachable or disagreed to participate. Out of 59 EO-PD patients from our database 21 were excluded because of DBS, 21 disagreed to participate and one was excluded due to insufficient temporal bone window. Twenty-two WD and 16 EO-PD patients participated in the study. The control group consisted of 24 healthy subjects with no neuropsychiatric disorder. All subjects signed informed consent and the study was approved by the Ethical Committee of General Teaching Hospital in Prague.

Information about initial clinical symptoms, abnormal serum ceruloplasmin concentration, urine copper excretion, liver copper concentration, and the presence of K-F ring at the time of diagnosis was retrieved from medical records.

Twenty WD patients were on a stable medication while two were *de novo* treatment naïve patients at the time of examination (Table 1). Fifteen PD patients were on a stable antiparkinsonian medication while one was treatment naïve. All PD patients were tested for *PARK2* mutations; heterozygous pathogenic mutation was found in one. Neurological impairment was assessed by the Unified Wilson's Disease Rating Scale (UWDRS) [21] in WD and by the Unified Parkinson's Disease Rating Scale, Part III (UPDRS-III) in EO-PD group respectively. Patients were examined on their usual symptomatic therapy. “Joint parkinsonism subscore” was calculated from items present jointly in both scales in order to compare the severity of parkinsonism in WD and EO-PD groups. This subscore consists of UPDRS-III except items 24, 30 and 31.

2.2. Magnetic resonance imaging

MRI was performed using 1.5 T whole body Philips Achieva system in EO-PD and WD patients. Standard spin echo T1w (resolution = 1.2 × 1.2 × 3 mm^3, TE = 15 ms, TR = 500 ms) and T2w (resolution = 0.5 × 0.5 × 2 mm^3, TE = 233 ms, TR = 2250 ms) sequences covering the whole brain were employed to quantify brain damage and generate anatomical images for TCS fusion. An experienced neuroradiologist blinded to the diagnosis quantified the MRI pathology. Degree of atrophy was graded as absent (0 points) mild (1 point) or severe (2 points) in three locations: 1) cerebellum and brainstem, 2) basal ganglia and subcortical region and 3) cortex. At that, presence of T2 hyperintensities in the caudate nucleus, putamen, globus pallidus, thalamus, mesencephalon, pons and T2 hypointensities in the NL, SN, and dentate nucleus were scored by 1 point each. The total sum of atrophy and signal changes build the composite MRI severity score (maximum 15 points) [22].

2.3. Transcranial sonography

The ultrasound system MyLab Twice (Esaote S.p.A., Genova, Italy) was equipped with the Virtual Navigation (MedCom GmbH, Darmstadt, Germany), which allows real-time image fusion of TCS and MRI images. The ultrasound scanner with a Reusable Tracking Bracket (CIVCO, Kalona, IA, USA) and sensor mount were used. The Virtual Navigator technology was implemented using an electromagnetic tracking system, composed of a transmitter and a small receiver, mounted on the ultrasound probe. SN was imaged in the axial mesencephalic plane (Fig. 1A) while NL and caudate nucleus (CN) were imaged in the axial thalamic plane (Fig. 1B) using the Fusion Imaging technique.

Following parameters were used: penetration depth of 16 cm, penetration high, dynamic range 7 (50 dB), frequency 1–4 MHz, enhancement 3, density 2, view 9, persistence 7, dynamic compression 0, gain 36%, grey map 0, S-view off, 2 focuses in 5 and 10 cm, mechanical index 0.9, tissue indices TIs 1.0, TIB 1.0 and TIC 2.1.

The butterfly-shaped structure of the mesencephalic brainstem and the region of SN in mesencephalic section and CN and LN in the thalamic section were depicted and images were saved in 8-bit grayscale DICOM format for offline analysis. Predefined elliptical ROIs were manually placed in the region of contralateral CN and LN and ipsilateral SN (Supplementary Figure). The echogenicity indices were calculated separately for SN, CN and LN from both right and left temporal bone windows using the B-Mode Assist software for digital image analysis [18,23]; the higher value of both measurements was used for analysis.

Standard visual assessment of SN and LN echogenicity [24] was also performed and results were compared with those obtained by digital image analysis. The mean SN echogenic area from both sides

Please cite this article in press as: J. Mašková, et al., Comparison of transcranial sonography-magnetic resonance fusion imaging in Wilson's and early-onset Parkinson's diseases, Parkinsonism and Related Disorders (2016), http://dx.doi.org/10.1016/j.parkreldis.2016.04.031

Table 1
Demography, clinical and TCS findings.

	WD	EO-PD	Control
Number of patients (females)	22 (11)	16 (9)	24 (16)
Age; mean ± SD (years)[a]	43.9 ± 8.7	42.2 ± 5.2	37.6 ± 10.3
Duration of disease; mean ± SD (years)[b]	17.1 ± 9.9	7.7 ± 4.7	–
Duration of therapy; mean ± SD (years)[b]	13.5 ± 7.2	3.8 ± 1.9	–
UPDRS-III subscore; mean; median (interquartile range)	–	21.3; 16.0 (12.0–32.0)	–
UWDRS neurologic subscore; mean; median (interquartile range)	19.6; 13.5 (7.0–30.5)	–	–
UWDRS/UPDRS-III joint parkinsonism subscore; mean; median (interquartile range)[c]	9.1; 4.5 (2.0–14.3)	14.9, 13.0 (9.0–21.0)	–
L-DOPA equivalent; mean ± SD (mg)	–	623.4 ± 453.2	–
Number of patients on d-PEN/Zinc/combination treatment	7/8/4	–	–
Composite MRI severity score; mean; median (interquartile range)[b]	5.9, 6.0 (2.0–8.5)	2.3, 2.0 (1.0–3.5)	–
TCS results			
SN echogenicity index; mean ± SD[d]	28.0 ± 4.6	39.8 ± 5.9	28.8 ± 4.9
NL echogenicity index; mean ± SD[e]	117.5 ± 37.0	61.6 ± 5.4	54.9 ± 11.2
CN echogenicity index; mean ± SD[f]	47.5 ± 16.5	39.6 ± 9.2	34.4 ± 7.4
SN echogenic area (cm^2); mean ± SD[d]	0.20 ± 0.03	0.26 ± 0.04	0.19 ± 0.03
Subject with abnormal SN echogenicity; n (%)[g]	4/22 (18%)	12/16 (75%)	3/24 (13%)
Subjects with abnormal NL echogenicity; n (%)[g]	15/22 (68%)	3/16 (19%)	3/24 (13%)
Established WD diagnostic methods			
Subjects with abnormal serum ceruloplasmin (<0.2 g/l); n (%)[g]	17/22 (77%)	2/15 (13%)	N.A.
Subjects with abnormal 24-h urine copper excretion (>1 μmol/24 h); n (%)[g]	21/22 (95%)	2/12 (15%)	N.A.
Subjects with positive K-F ring; n (%)[g]	15/22 (68%)	0/12 (0%)	N.A.
Subjects with abnormal liver copper concentration (>250 μg/g dry tissue); n (%)	20/20 (100%)	N.A.	N.A.
Subjects with confirmed pathogenic mutation of *ATP7B*; n (%)[h]	16/22 (73%)	N.A.	N.A.

Abbreviations: WD – Wilson disease, EO-PD, early-onset Parkinson's disease, UWDRS – Unified Wilson's Disease Rating Scale, UPDRS-III – Unified Parkinson's Disease Rating Scale, Part III; d-PEN – d-penicillamine, SN – substantia nigra, NL – lentiform nucleus, CN – caudate nucleus, N.A. – not available.

[a] $p < 0.05$ WD compared to controls (ANOVA and Tukey's post-hoc test).
[b] $p < 0.01$ WD compared to EO-PD (Mann-Whitney *U* test).
[c] $p < 0.05$ EO-PD compared to WD (Mann-Whitney *U* test).
[d] $p < 0.0001$ EO-PD compared to WD and controls (ANOVA and Tukey's post-hoc test).
[e] $p < 0.0001$ WD compared to EO-PD and controls (ANOVA and Tukey's post-hoc test).
[f] $p < 0.01$ WD compared to controls (ANOVA and Tukey's post-hoc test).
[g] $p < 0.001$ (Fischer's exact test).
[h] Sequencing of coding regions of the *ATP7B* gene revealed homozygous p.[His1069Gln] mutation in 10 and compound heterozygous mutation p.[His1069Gln] and: [Gly1176Arg] in 1; [Arg778Gly] in 1; [Val1262Phe] in 1; [Gly710Ser] in 2; and [Ala1135fs] in 1 subject. Homozygous p.[Lys1248Thrfs*83] mutation was detected in 1 subject.

was compared in WD, EO-PD, and control group. In the calculation of sensitivity/specificity for differentiation of WD and EO-PD, the larger echogenic area of the two sides was employed while SN hyperechogenicity was defined as echogenic area >0.24 cm^2. Echogenic signals from NL in comparison to surrounding tissue were assessed visually and rated as “normal” or “hyperechogenic”. The echogenicity of NL was regarded as abnormal when hyperechogenic signal was detected at least on one side. A single sonographer who was blinded to the patients' diagnoses but not to movement disorders symptoms performed examinations and image analyses.

2.4. Statistics

The Shapiro-Wilk test was used for normality testing. Data with a normal distribution are reported as mean ± standard deviation. Variables not fitting the normal distribution are presented as a mean, median and interquartile range. Comparisons between two groups were performed using the Mann-Whitney *U* test. Group differences among WD, EO-PD, and control groups were tested using one-way ANOVA with post-hoc Tukey's test. Receiver operating characteristic (ROC) curves were plotted and sensitivity/specificity was calculated for determined cut-off points of SN, NL and CN echogenicity. Sensitivities/specificities were calculated from contingency tables for serum ceruloplasmin, 24-h urine copper excretion, presence of K-F ring, and visually assessed SN and NL hyperechogenicity; frequencies were compared by Fischer's exact test. Dependence of variables was assessed using Pearson correlation coefficient. All reported p-values are two-tailed. Statistical evaluations were performed using the GraphPad Prism version 6 (GraphPad Software, San Diego, CA, USA).

3. Results

3.1. Clinical assessment

Demographic and medical data are shown in Table 1. The age-range was wider and mean age slightly lower in control subjects but age and echogenicity indices in examined structures were not significantly correlated (data not shown), in accordance with a population study examining SN echogenic area [9]. Twenty-one WD subjects fulfilled the clinical criteria for hypokinetic-rigid syndrome (i.e. presence of akinesia and one of the following: rigidity, tremor or postural instability). Parkinsonian symptoms were more severe in the EO-PD group as documented by higher joint parkinsonism score ($p < 0.05$). Four WD cases initially manifested with isolated parkinsonism and one EO-PD case manifested with leg dystonia. Sensitivities/specificities for WD and EO-PD differentiation were calculated for established screening methods reaching 77/88% for serum ceruloplasmin concentration, 95/83% for 24-h urinary copper excretion and 68/100% for K-F ring.

3.2. TCS findings

The EO-PD group exhibited SN hyperechogenicity and the WD group NL hyperechogenicity in comparison with the control group (Fig. 2). Group analysis of digital image analysis results was significant for both brain areas, SN ($F[2, 59] = 30.0$, $p < 0.0001$) and NL ($F[2, 59] = 47.2$, $p < 0.0001$). Post-hoc Tukey's test showed that SN echogenicity in the EO-PD group was significantly higher than in the WD ($p < 0.0001$) and control ($p < 0.0001$) groups and that NL echogenicity was significantly higher in the WD group compared to the EO-PD ($p < 0.0001$) and controls ($p < 0.0001$). Similar pattern as

Please cite this article in press as: J. Mašková, et al., Comparison of transcranial sonography-magnetic resonance fusion imaging in Wilson's and early-onset Parkinson's diseases, Parkinsonism and Related Disorders (2016), http://dx.doi.org/10.1016/j.parkreldis.2016.04.031

Fig. 1. Typical TCS findings in WD patient with corresponding MRI images using the fusion imaging technique. A) axial mesencephalic plane showing normal echogenicity of a substantita nigra; B) axial thalamic plane showing hyperechogenic lentiform nucleus. Numbers indicate following anatomical structures: 1 – mesencephalon; 2 – temporal lobe; 3 – cerebellum; 4 – third ventricle; 5 – frontal horn of lateral ventricle; 6 – caudate nucleus; 7 – lentiform nucleus; 8 – insula; 9 – occipital horn of lateral ventricle.

in NL, but with weaker significance, was observed also in CN (Table 1).

The cut-off value for SN and LN echogenicity indices were determined 33.7 and 71.9 respectively. SN hyperechogenicity reached sensitivity 93.8%, specificity 90.9% and area under the ROC curve (AUC) of 0.972 (95% confidence interval = 0.928–1.00, $p < 0.0001$), while NL hyperechogenicity reached sensitivity 95.5%, specificity 93.8% and AUC of 0.992 (95% confidence interval = 0.973–1.00, $p < 0.0001$) for a differentiation of WD and EO-PD (Fig. 3).

The visual assessment of SN echogenicity detected significantly larger mean SN echogenic area in EO-PD subjects compared to WD ($p < 0.0001$) and controls ($p < 0.0001$). The sensitivity/specificity of visually assessed hyperechogenicity was 75/82% in SN and 68/81% in NL for WD and EO-PD differentiation.

Please cite this article in press as: J. Mašková, et al., Comparison of transcranial sonography-magnetic resonance fusion imaging in Wilson's and early-onset Parkinson's diseases, Parkinsonism and Related Disorders (2016), http://dx.doi.org/10.1016/j.parkreldis.2016.04.031

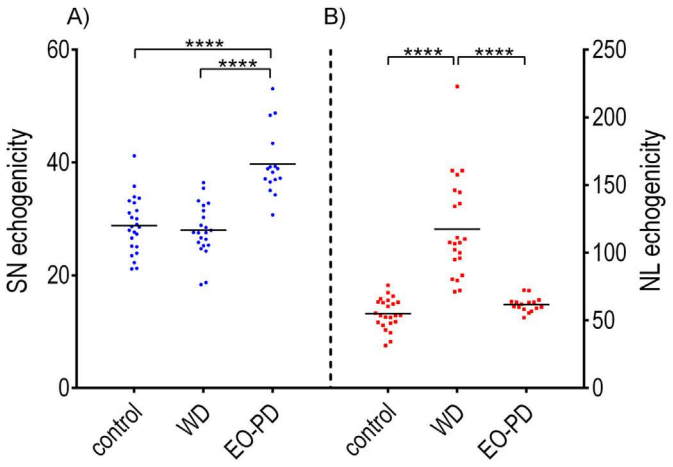

Fig. 2. Echogenicity index in A) substantia nigra (SN) and B) lentiform nucleus (NL) in control subjects, Wilson disease (WD) and early-onset Parkinson's disease (EO-PD) groups. Y-axes are differently adjusted for SN and NL values respectively. Echogenicity index in CN exhibited similar pattern as in NL and is thus not depicted in this graph.

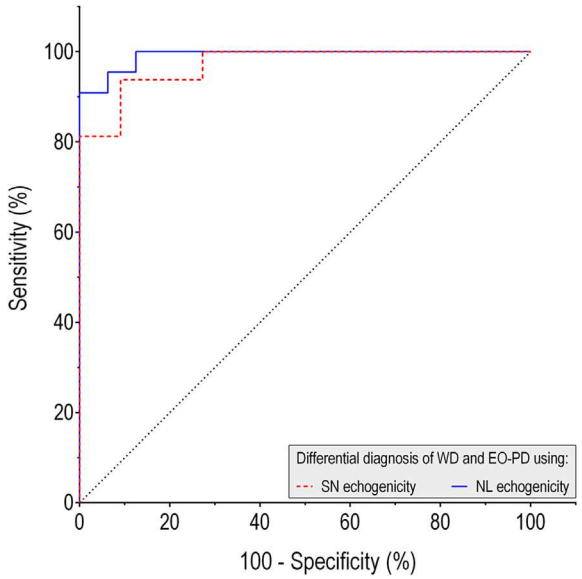

Fig. 3. Receiver operating characteristic (ROC) of substantia nigra (SN, dashed line) and lentiform nucleus (NL, solid line) echogenicity in the differential diagnosis of Wilson's disease and early-onset Parkinson's disease.

3.3. Correlation between TCS, MRI, and clinical parameters

TCS findings of two *de novo* WD patients did not differ from patients on chronic treatment (NL echogenicity index 134.2 and 107.5 vs. 117.1 ± 38.6, $p = 0.70$). Furthermore, we did not find correlation between the NL echogenicity index and age ($r = -0.36$, $p = 0.10$), disease duration ($r = -0.32$, $p = 0.14$), treatment duration ($r = -0.21$, $p = 0.36$) or UWDRS score ($r = 0.36$, $p = 0.10$) in the WD group. In EO-PD group, we did not observe correlation between SN echogenicity index and age ($r = 0.06$, $p = 0.84$), disease duration ($r = -0.14$, $p = 0.61$) and UPDRS-III score ($r = 0.02$, $p = 0.93$).

The composite MRI severity score was higher in the WD compared to the EO-PD group ($p < 0.01$) (Table 1). MRI signal in the NL in T2w images was normal in six, hypointense in 12, while T2 hyperintense signal in the putamen was present in 13 WD patients. Out of the group of six WD patients with normal MR signal in NL, none had NL echogenicity index within the normal range. NL echogenicity index was higher in WD patients presenting compared to those not presenting with T2 hyperintense signal in the putamen (140.4 ± 13.6 vs 106.9 ± 8.2, $p = 0.03$) while no difference in NL echogenicity index was observed between patients presenting and not presenting T2 hypointense signal in NL (113.2 ± 9.5 vs 124.5 ± 12.1, $p = 0.70$). T2 hypointense signal in the SN and/or T2 hyperintense signal in the mesencephalic white matter was present in 13 WD patients. In the EO-PD group, NL was rated as hypointense in four patients while hypointense SN was not found in any patient.

4. Discussion

The results of our study confirmed that the NL and SN echogenicity indices examined by digital image analysis of TCS-MRI fusion images are sensitive and specific markers of WD and EO-PD. The hyperechogenicity of SN in the EO-PD group was detected in 93.8% cases, in accordance with previous TCS studies. In the control group slightly increased NL and SN echogenicities were found in about one tenth of subjects without any clinical correlate. This proportion of healthy subjects with SN hyperechogenicity is consistent across studies and their potential risk of developing parkinsonism is discussed [6].

The NL echogenicity index was abnormal in 95.5% of WD patients. Increased echogenicity index of CN in WD patients was less constant than NL hyperechogenicity. Sensitivity and specificity of NL hyperechogenicity were comparable to routinely used screening methods, i.e. serum ceruloplasmin, urinary copper and K-F ring supporting its potential value as a screening examination of WD. Notably, K-F ring was not detectable in 32% of our WD cases in whom diagnosis was confirmed by genetic examination and/or increased liver copper concentration. This finding, which is in line with several recent studies showing that significant proportion of neurological WD patients may lack the K-F ring [3,25,26], advocates the utility of other screening investigations.

SN echogenicity in WD patients was similar as in control subjects, yielding approximately 10% of subjects with hyperechogenicity. This is in contrast to previous studies showing >50% prevalence of SN hyperechogenicity in WD [12,13].

Our finding of normal SN echogenicity in WD patients is surprising since the majority of the WD patients were affected by parkinsonism. Previous studies suggested a link between parkinsonism in WD and variable combination of pre- and postsynaptic damage of the nigrostriatal pathway [27]. Moreover, 13 WD patients had T2 hypointensity in SN and/or T2 hyperintensity in the mesencephalic white matter tracts. These results suggest that, in the case of SN, its microstructural damage depicted on MRI may not invariably affect its echogenicity.

With respect to the echogenicity changes of NL and CN, our results are comparable to two previously published studies [12,13]. The first of the studies found NL hyperechogenicity in 100% of neurological WD patients and a significant correlation between NL hyperechogenicity and clinical severity [12]. The second one found NL hyperechogenicity in 81.6% of neurological WD patients and detected a correlation between SN hyperechogenicity and clinical severity [13].

In contrast to these studies, we did not find any correlation between TCS findings, clinical severity and duration of disease or treatment. Taking these contradictory results into consideration, TCS probably cannot be used as a reliable marker for longitudinal follow-up of chelating therapy or disability prognosis.

There are several factors, which may contribute to disparate SN echogenicity results. For more accurate anatomical delineation of examined structures we used real-time MRI fusion imaging

Please cite this article in press as: J. Mašková, et al., Comparison of transcranial sonography-magnetic resonance fusion imaging in Wilson's and early-onset Parkinson's diseases, Parkinsonism and Related Disorders (2016), http://dx.doi.org/10.1016/j.parkreldis.2016.04.031

technology. Although not yet validated in neurological applications, fusion imaging may allow for better identification of brain structures, particularly in oblique imaging planes. Thus, echogenicity indices might be more accurate when using this technique. In addition, we also applied newly developed software for digital analysis of brain structures echogenicity that automatically accounts for the quality of the bone window, different depth, and shades of grey. Its usage eliminates the incorrect manual evaluation of echogenicity and increases sensitivity and comparability [18,23]. Accordingly, sensitivity and specificity for WD and EO-PD differentiation were lower in our cohort when visual analysis of echogenicity was employed.

Although TCS is an easy and cheap examination, it has several limitations. Only one patient (2.6%) from the studied group had to be excluded due to insonability. However, in large population studies insufficient temporal bone window, particularly for NL assessment, is found in more than 10% of subjects [9]. In addition, MRI-TCS fusion with subsequent digital image analysis with duration of 20–30 min is more time consuming compared to standard visual analysis, which may limit its practicability. Further studies should investigate whether similar results can be obtained without MRI-TCS fusion when digital image analysis algorithm would be implemented in the software of routine ultrasound devices. This could decrease the examination duration to 10 min.

Interpretation of TCS findings is hampered by the lack of understanding of neuropathological underpinnings of tissue hyperechogenicity. The widespread hypothesis suggests its connection with the accumulation of iron and copper. Presumed dependence of tissue echogenicity on iron concentration [28] implies that TCS hyperechogenicity should correlate with MRI T2/T2* hypointensity, predominantly caused by paramagnetic iron species [29]. Contrary to this assumption, the degree of NL hyperechogenicity was related to putaminal T2 hyperintensity rather than to T2 hypointensity in NL suggesting that echogenicity is not only determined by iron concentration. In addition, we found NL hyperechogenicity in all WD patients with normal MR signal in this area confirming previous findings that TCS can bring complementary information to MRI [14,15,30]. The echogenicity changes could be also influenced by copper as documented in a post-mortem study on WD brains showing a correlation between echogenicity and copper concentration in NL [11]. Since MRI cannot reliably depict copper [29], we cannot support nor foreclose its effect on tissue echogenicity in our patients. To sum up, the underpinnings of echogenicity contrast in TCS examination are complex and depend not only on metal accumulation but also on associated pathological microstructural tissue changes.

Despite the limitation of the small number of patients, the sensitivity and specificity of the results are obvious and our findings are in good accordance with previously published studies in PD and WD patients. However, in this proof of concept study we did not examine only *de novo* patients, not all the patients with WD have had isolated parkinsonism, and disease duration was different between groups. Therefore, additional studies with untreated *de novo* patients are needed to confirm the utility of TCS in the differential diagnosis of WD and EO-PD.

With regard to the results above and previously performed studies, we can conclude that TCS findings in WD and EO-PD are potentially helpful as screening biomarkers in early-onset parkinsonism. For the future, it could be efficient to include TCS abnormality into supportive neuroimaging criteria for WD.

Conflict of interest

None of the authors report a conflict of interest with respect to financial or personal relationships with organizations that may have an influence on this work.

Acknowledgements

This study was supported by Ministry of Health of the Czech Republic, grant no. 15-25602A and Charles University in Prague, PRVOUK P26/LF1/4 and UNCE 204011/12; and RVO-VFN64165.

Appendix A. Supplementary data

Supplementary data related to this article can be found at http://dx.doi.org/10.1016/j.parkreldis.2016.04.031.

References

[1] P. Dusek, T. Litwin, A. Czlonkowska, Wilson disease and other neurodegenerations with metal accumulations, Neurol. Clin. 33 (2015) 175–204.
[2] P. Ferenci, Pathophysiology and clinical features of Wilson disease, Metab. Brain Dis. 19 (2004) 229–239.
[3] J. Youn, J.S. Kim, H.T. Kim, J.Y. Lee, P.H. Lee, C.S. Ki, J.W. Cho, Characteristics of neurological Wilson's disease without Kayser-Fleischer ring, J. Neurol. Sci. 323 (2012) 183–186.
[4] J. Bennett, S.H. Hahn, Clinical molecular diagnosis of Wilson disease, Semin. Liver Dis. 31 (2011) 233–238.
[5] R. Abdullah, I. Basak, K.S. Patil, G. Alves, J.P. Larsen, S.G. Moller, Parkinson's disease and age: the obvious but largely unexplored link, Exp. Gerontol. 68 (2015) 33–38.
[6] U. Walter, D. Dressler, A. Wolters, M. Wittstock, R. Benecke, Transcranial brain sonography findings in clinical subgroups of idiopathic Parkinson's disease, Mov. Disord. 22 (2007) 48–54.
[7] U. Walter, D. Dressler, T. Probst, A. Wolters, M. Abu-Mugheisib, M. Wittstock, R. Benecke, Transcranial brain sonography findings in discriminating between parkinsonism and idiopathic Parkinson disease, Arch. Neurol. 64 (2007) 1635–1640.
[8] J.M. Hagenah, K. Hedrich, B. Becker, P.P. Pramstaller, G. Seidel, C. Klein, Distinguishing early-onset PD from dopa-responsive dystonia with transcranial sonography, Neurology 66 (2006) 1951–1952.
[9] P. Mahlknecht, K. Seppi, H. Stockner, M. Nocker, C. Scherfler, S. Kiechl, J. Willeit, C. Schmidauer, A. Gasperi, G. Rungger, W. Poewe, Substantia nigra hyperechogenicity as a marker for Parkinson's disease: a population-based study, Neurodegener. Dis. 12 (2013) 212–218.
[10] D. Berg, S. Behnke, K. Seppi, J. Godau, S. Lerche, P. Mahlknecht, I. Liepelt-Scarfone, C. Pausch, N. Schneider, A. Gaenslen, K. Brockmann, K. Srulijes, H. Huber, I. Wurster, H. Stockner, S. Kiechl, J. Willeit, A. Gasperi, K. Fassbender, T. Gasser, W. Poewe, Enlarged hyperechogenic substantia nigra as a risk marker for Parkinson's disease, Mov. Disord. 28 (2013) 216–219.
[11] U. Walter, M. Skowronska, T. Litwin, G.M. Szpak, K. Jablonka-Salach, D. Skoloudik, E. Bulska, A. Czlonkowska, Lenticular nucleus hyperechogenicity in Wilson's disease reflects local copper, but not iron accumulation, J. Neural Transm. Vienna 121 (2014) 1273–1279.
[12] U. Walter, K. Krolikowski, B. Tarnacka, R. Benecke, A. Czlonkowska, D. Dressler, Sonographic detection of basal ganglia lesions in asymptomatic and symptomatic Wilson disease, Neurology 64 (2005) 1726–1732.
[13] M. Svetel, M. Mijajlovic, A. Tomic, N. Kresojevic, T. Pekmezovic, V.S. Kostic, Transcranial sonography in Wilson's disease, Park. Relat. Disord. 18 (2012) 234–238.
[14] R. Martinez-Fernandez, N. Caballol, M. Gomez-Choco, MRI and transcranial sonography findings in Wilson's disease, Mov. Disord. 28 (2013) 740.
[15] M.C. Ricciardi, G. Sirimarco, E. Vicenzini, C. Zuco, G. Meco, V. Di Piero, G.L. Lenzi, Transcranial sonographic findings in Wilson disease, J. Ultrasound Med. 29 (2010) 1143–1145.
[16] S. Sinha, A.B. Taly, S. Ravishankar, L.K. Prashanth, K.S. Venugopal, G.R. Arunodaya, M.K. Vasudev, H.S. Swamy, Wilson's disease: cranial MRI observations and clinical correlation, Neuroradiology 48 (2006) 613–621.
[17] S. Schreiber, G. Sakas, V. Kolev, S. Beni, Fusion imaging in neurosonology: clinician's questions, technical potentials and applicability, Biomed. Eng. Lett. 4 (2014) 347–354.
[18] D. Skoloudik, M. Jelinkova, J. Blahuta, P. Cermak, T. Soukup, P. Bartova, K. Langova, R. Herzig, Transcranial sonography of the substantia nigra: digital image analysis, AJNR – Am. J. Neuroradiol. 35 (2014) 2273–2278.
[19] R.J. Wong, R. Gish, M. Schilsky, C. Frenette, A clinical assessment of Wilson disease in patients with concurrent liver disease, J. Clin. Gastroenterol. 45 (2011) 267–273.
[20] A.J. Hughes, S.E. Daniel, L. Kilford, A.J. Lees, Accuracy of clinical diagnosis of idiopathic Parkinson's disease: a clinico-pathological study of 100 cases, J. Neurol. Neurosurg. Psychiatry 55 (1992) 181–184.
[21] B. Leinweber, J.C. Moller, A. Scherag, U. Reuner, P. Gunther, C.J. Lang, H.H. Schmidt, C. Schrader, O. Bandmann, A. Czlonkowska, W.H. Oertel, H. Hefter, Evaluation of the unified Wilson's disease rating scale (UWDRS) in German patients with treated Wilson's disease, Mov. Disord. 23 (2008)

54–62.
[22] N.A. Frota, E.R. Barbosa, C.S. Porto, L.T. Lucato, C.R. Ono, C.A. Buchpiguel, P. Caramelli, Cognitive impairment and magnetic resonance imaging correlations in Wilson's disease, Acta Neurol. Scand. 127 (2013) 391–398.
[23] J. Blahuta, T. Soukup, M. Jelinkova, P. Bartova, P. Cermak, R. Herzig, D. Skoloudik, A new program for highly reproducible automatic evaluation of the substantia nigra from transcranial sonographic images, Biomed. Pap. Med. Fac. Univ. Palacky. Olomouc Czech Repub. 158 (2014) 621–627.
[24] U. Walter, D. Skoloudik, Transcranial sonography (TCS) of brain parenchyma in movement disorders: quality standards, diagnostic applications and novel technologies, Ultraschall Med. 35 (2014) 322–331.
[25] V. Mihaylova, T. Todorov, H. Jelev, I. Kotsev, L. Angelova, O. Kosseva, G. Georgiev, R. Ganeva, S. Cherninkova, L. Tankova, A. Savov, I. Tournev, Neurological symptoms, genotype-phenotype correlations and ethnic-specific differences in Bulgarian patients with Wilson disease, Neurologist 18 (2012) 184–189.
[26] M. Fenu, M. Liggi, E. Demelia, O. Sorbello, A. Civolani, L. Demelia, Kayser-Fleischer ring in Wilson's disease: a cohort study, Eur. J. Intern. Med. 23 (2012) e150–156.
[27] H. Barthel, W. Hermann, R. Kluge, S. Hesse, D.R. Collingridge, A. Wagner, O. Sabri, Concordant pre- and postsynaptic deficits of dopaminergic neurotransmission in neurologic Wilson disease, AJNR – Am. J. Neuroradiol. 24 (2003) 234–238.
[28] D. Berg, W. Roggendorf, U. Schroder, R. Klein, T. Tatschner, P. Benz, O. Tucha, M. Preier, K.W. Lange, K. Reiners, M. Gerlach, G. Becker, Echogenicity of the substantia nigra: association with increased iron content and marker for susceptibility to nigrostriatal injury, Arch. Neurol. 59 (2002) 999–1005.
[29] P. Dusek, M. Dezortova, J. Wuerfel, Imaging of iron, Int. Rev. Neurobiol. 110 (2013) 195–239.
[30] W. Hermann, Morphological and functional imaging in neurological and non-neurological Wilson's patients, Ann. N. Y. Acad. Sci. 1315 (2014) 24–29.

Please cite this article in press as: J. Mašková, et al., Comparison of transcranial sonography-magnetic resonance fusion imaging in Wilson's and early-onset Parkinson's diseases, Parkinsonism and Related Disorders (2016), http://dx.doi.org/10.1016/j.parkreldis.2016.04.031

Ultrasound in Med. & Biol., Vol. 00, No. 00, pp. 1–7, 2019

0301-5629/$ - see front matter

https://doi.org/10.1016/j.ultrasmedbio.2019.12.013

● *Original Contribution*

DIGITIZED IMAGE ANALYSIS OF INSULA ECHOGENICITY DETECTED BY TCS-MR FUSION IMAGING IN WILSON'S AND EARLY-ONSET PARKINSON'S DISEASES

David Školoudík,*,† Jana Mašková,* Petr Dušek,*,‡ Jiří Blahuta,§ Tomáš Soukup,§ Andrea Burgetová,‡ and Petra Bártová¶

* Department of Neurology and Center of Clinical Neuroscience, First Faculty of Medicine, Charles University and General University Hospital in Prague, Prague, Czech Republic; † Department of Neurology, University Hospital Ostrava, Ostrava, Czech Republic; ‡ Department of Radiology, First Faculty of Medicine, Charles University and General University Hospital in Prague, Prague, Czech Republic; § Institute of Computer Science, Faculty of Philosophy and Science, Silesian University in Opava, Opava, Czech Republic; and ¶ Department of Neurology, Ostrava University Medical Faculty and University Hospital Ostrava, Ostrava, Czech Republic

(*Received* 7 *July* 2019; *revised* 2 *November* 2019; *in final from* 11 *December* 2019)

Abstract—Transcranial sonography (TCS) can reveal pathology in brain structures including insula. This study compared insula echogenicity among 22 patients with Wilson's disease (WD), 21 patients with early-onset Parkinson's disease (EO-PD) and 24 healthy patients. Echogenicity of predefined brain structures (insula, lentiform nucleus, caudate nucleus, substantia nigra and raphe nuclei) was evaluated using digitized analysis of TCS fusion imaging with magnetic resonance. Cortical, subcortical and cerebellar atrophy and ventricle diameters were determined from magnetic resonance images. The mean echogenicity index of insula did not differ between males and females ($p = 0.92$), but the echogenicity of insula was higher in patients with WD than in patients with EO-PD and healthy patients ($p < 0.05$). The substantia nigra echogenicity was higher in patients with EO-PD, and lentiform nucleus echogenicity was higher in patients with WD ($p < 0.05$). The echogenicity of insula correlated with lentiform nucleus echogenicity ($r = 0.75$) but not with age ($r = -0.14$), disease duration ($r = -0.36$), symptom severity ($r = 0.28$), cortical ($r = 0.11$) nor subcortical ($r = 0.05$) atrophy. (E-mail: skoloudik@hotmail.com)

Key Words: **Wilson's disease, Parkinson's disease, Transcranial sonography, Magnetic resonance, Echogenicity.**

INTRODUCTION

Transcranial sonography (TCS) is a useful tool for detecting pathologies of the brain parenchyma based on changes in echogenicity in brain structures including substantia nigra (SN), brainstem raphe, caudate nucleus, lentiform nucleus (LN), or dentate nucleus (Walter and Školoudík 2014). This can aid in the diagnosis of and differentiation among brain diseases such as Parkinson's disease (PD) and other Parkinsonian syndromes, dystonia, depression, panic disorder, Wilson's disease (WD) and Huntington disease (Walter et al. 2007; Berg et al. 2008; Walter and Školoudík 2014). However, TCS has lower spatial resolution than other neuroimaging methods such as computed tomography (CT) or magnetic resonance (MR). It is also limited by the quality of the bone window and is dependent on sonographer skills (Školoudík and Walter 2010; Walter and Školoudík 2014).

These drawbacks can be overcome by fusion imaging (with MR or CT) using Virtual Navigator and digitized image analysis (Blahuta et al. 2011, 2014; Laganá et al. 2011, 2013; Forzoni et al. 2012; Školoudík et al. 2014), which has not only improved the assessment of visually detectable structures on TCS images but has also enabled evaluation of the echogenicity of other brain structures such as insula, which can be segmented only with the aid of a fused MR image (Školoudík et al. 2016). An earlier study has shown that the echogenicity of insula can be reliably measured with low intra- and inter-rater variability by TCS-MR fusion imaging (Školoudík et al. 2016). However, there have been no studies to date assessing the echogenicity of insula in various diseases.

Address correspondence to: Prof. David Školoudík, MD, PhD, FESO, FEAN, Department of Neurology, University Hospital Ostrava, 17. listopadu 1790/5, CZ-70852 Ostrava, Czech Republic. E-mail: skoloudik@hotmail.com

Accumulation of iron, manganese, copper, or other substrates; neuronal loss; gliosis; and other structural changes can cause variations in the echogenicity of brain parenchyma (Berg et al. 1999; Behnke et al. 2009; Walter et al. 2014; Walter and Školoudík 2014; Ghassaban et al. 2019). However, pathologic processes leading to changes in the echogenicity of various brain structures are not fully understood.

PD and WD are characterized by increases in echogenicity of particular brain structures that are detectable by TCS—for example, an increased SN echogenicity in PD and hyperechogenic LN in WD resulting from cerebral accumulation of metals leading to brain parenchymal damage (Berg et al. 1999; Behnke et al. 2009; Walter et al. 2014; Walter and Školoudík 2014; Yu et al. 2018). Thus, LN and SN echogenicity can serve as sensitive diagnostic markers in these disorders (Berg et al. 1999; Behnke et al. 2009; Mijajlovic et al. 2014; Walter et al. 2014; Walter and Školoudík 2014; Yu et al. 2018).

In this study, we compared insula echogenicity among patients with WD and patients with early-onset (EO)-PD and healthy patients by TCS-MR fusion imaging, using Virtual Navigator and digitized image analysis. We also carried out an exploratory correlation analysis to identify clinical and imaging factors associated with the echogenicity of insula.

MATERIALS AND METHODS

Patients

Data for this study were acquired during the same session on the same patients (22 patients with WD and 16 patients with early-onset Parkinson's disease (EO-PD) as in our earlier TCS study (Mašková et al. 2016), although 1 patient with WD and 7 additional patients with EO-PD were included. Inclusion criteria were a neurologic form of WD with a diagnosis established according to Leipzig criteria for the WD group, and diagnosis according to the UK Parkinson's Disease Society Brain Bank criteria and age at onset $\leq$40 y for the EO-PD group. The control group had 24 healthy patients with no neuropsychiatric disorders. For all groups, an insufficient temporal bone window for TCS examination was an exclusion criterion. All patients provided written, informed consent before their participation in the study, and the study protocol was approved by the Ethical Committee of the General Teaching Hospital in Prague, Czech Republic.

Neurologic impairment was assessed using the Unified Wilson's Disease Rating Scale (UWDRS) in patients with WD and using the Unified Parkinson's Disease Rating Scale, Part III (UPDRS III) in patients with EO-PD. Patients were examined while receiving their usual symptomatic therapy.

MR imaging

MR images were acquired using a 1.5 T whole-body Achieva scanner (Philips, Eindhoven, The Netherlands). Standard spin echo T1 w (spatial resolution = $1.2 \times 1.2 \times 3$ mm^3, echo time (TE) = 15 ms, repetition time (TR) = 500 ms) and T2 w (spatial resolution = $0.5 \times 0.5 \times 2$ mm^3, TE = 233 ms, TR = 2250 ms) sequences covering the entire brain were used to quantify brain damage and generate anatomic images for TCS fusion. The insular cortex was clearly depicted in the axial T2 w sequences in 6−8 voxels in the latero-lateral direction and 10 slices (expected thickness 3−4 mm and extends >20 mm in rostro-caudal direction). The degree of brain atrophy on MR images was visually graded as absent (0 points), mild (1 point), or severe (2 points) in the following 3 locations: (i) cerebellum and brainstem, (ii) basal ganglia and subcortical region and (iii) cortex. The grading was carried out by an experienced neuroradiologist blinded to patients' diagnosis. Measurement of the third ventricle width was performed in the axial T2-weighted images in the middle of the anterior-posterior direction where the largest width of the ventricle was measured. Measurement of the fourth ventricle width was performed in the axial T2-weighted images in the largest width of the ventricle. All measurements were performed using the scanner software.

Transcranial sonography

The ultrasound system was equipped with the Virtual Navigation (Esaote S.p.A., Genoa, Italy, and MedCom GmbH, Darmstadt, Germany) option, which allows real-time image fusion of TCS and MR images. The ultrasound scanner Esaote MyLab Twice (Esaote S.p.A.) with a 2.5-MHz phased-array transducer (PA240), 639-039 CIVCO Reusable Tracking Bracket (CIVCO, Kalona, IA, USA) and sensor mount was used. Virtual Navigator procedures were implemented using an electromagnetic tracking system composed of a transmitter and a small receiver mounted on the ultrasound probe. The transmitter position—considered as the basis of the reference system—was fixed through a support, and the receiver provided the position and orientation of the ultrasound probe in relation to the transmitter. A proper head support was also used to keep the subject's head as steady as possible. Patients were examined in the supine position on a horizontal bed with 0° tilt.

After uploading the MR images in Digital Imaging and Communications in Medicine format to the Virtual Navigator, eight facial markers were used in all patients for fusion imaging and visualization of brain structures. Three internal markers were then used for a fine tuning to obtain a proper fusion. Transverse TCS images and corresponding MR images of the insula in the axial thalamic plane were acquired using both left and right transtemporal approaches (Fig. 1).

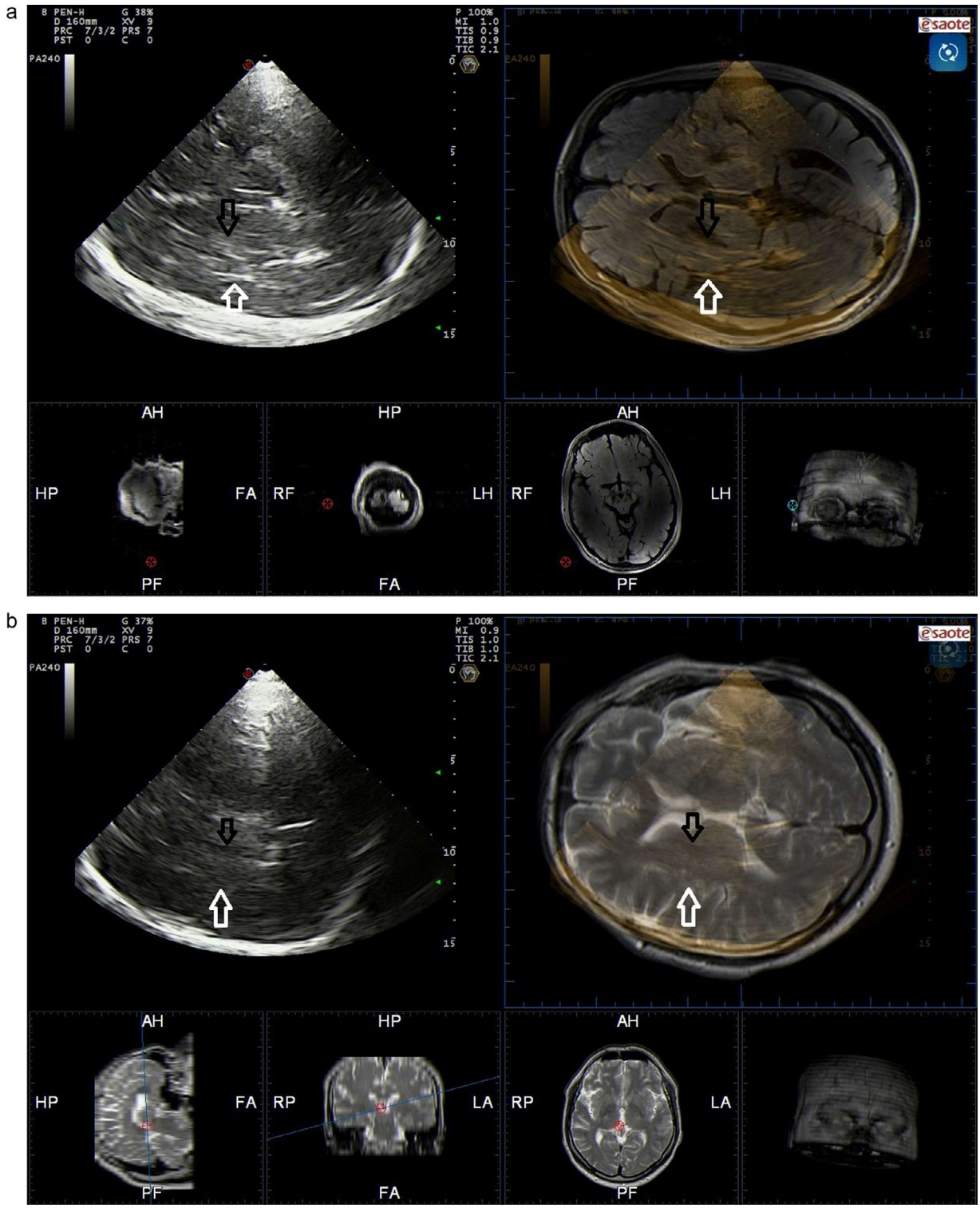

Fig. 1. Fusion imaging of transcranial sonography and magnetic resonance in the thalamic plane. (a) Increased echogenicity of lentiform nucleus and insula in patient with Wilson's disease. (b) Normal echogenicity of lentiform nucleus and insula in patient with early onset Parkinson's disease.

The examination was performed through both the right and left temporal bone window with the following parameters: a penetration depth of 16 cm, high penetration, dynamic range = 7 (50 dB), frequency = 1−4 MHz, enhancement = 3, density = 2, view = 9, persistence = 7, dynamic compression = 0, gain = 36%, gray map = 0, S view off, two focuses at 5 and 10 cm, mechanical index = 0.9 and the following tissue indices: thermal index for soft tissue = 1.0, thermal index for bone = 1.0 and thermal index for cranial bone 2.1. The TCS examination of all patients were performed with the exact same settings.

All images were saved in Digital Imaging and Communications in Medicine format. The B-Mode Assist tool and specific elliptical regions of interest were used for the measurement of echogenicity index of insula (area: 196 mm^2), SN (area: 50 mm^2), LN (area: 200 mm^2), caudate nucleus (area: 140 mm^2) and raphe nuclei (area: 40 mm^2) (Blahuta et al. 2014; Školoudík et al. 2014, 2016; Šilhán et al. 2015; Mašková et al. 2016). The higher of the 2 measured values for each structure was used for the analysis. The reproducibility of the insula echogenicity index measurement was calculated in an earlier study and reached intra-rater/inter-rater intra-class correlation coefficients of 0.995 (95% confidence interval [CI]: 0.993−0.997) / 0.937 (95% CI: 0.910−0.956) and Spearman's rank correlation coefficients of r = 0.993 / r = 0.921, respectively (Školoudík et al. 2016). The sonographer (D.Š.) was blinded to the patients' diagnosis but not to their movement disorder symptoms.

Statistics

The sample size of the study was based on an expected 30% difference in the echogenicity index of insula between groups. Pre-study calculations showed that a minimum of 23 patients in each group were needed to be screened to the study to reach a statistically significant difference with an α value of 0.05 (two-tailed) and β value of 0.8 (21 patients in each group), assuming that 10% of these patients (2 patients) would be excluded because of an insufficient bone window.

The Shapiro-Wilk test was used for normality testing. Data with a normal distribution are reported as mean ± standard deviation. Non-normally distributed variables are presented as a mean, median and interquartile range. Comparisons between two groups were performed with the Mann-Whitney *U* test. The Kruskal-Wallis test was used for comparison among three groups followed by Bonferroni multiple comparison test comparing all pairs. Differences among the WD, EO-PD and control groups were evaluated by one-way analysis of variance.

The dependence of variables was assessed using the Spearman's correlation coefficient. Bilateral measurements of insula, substantia nigra, caudate nucleus and LN were used for statistical evaluation. All reported *p* values are two-tailed. All tests were carried out at an α level of significance of 0.05. Data were analyzed using SPSS v.22.0 software (IBM Corp., Armonk, NY, USA).

RESULTS

Of the 70 patients screened for the study (23 patients with WD and 23 patients with EO-PD and 24 healthy controls), 3 (1 patient with WD and 2 patients with EO-PD) were excluded from analysis because of an insufficient bone window. Demographic and medical data of patients included in the analysis are presented in Table I. The mean echogenicity index of insula did not differ significantly between males and females (79.99 ± 29.07 vs. 80.78 ± 32.81; $p = 0.919$).

Echogenicity of insula was higher in patients with WD (103.92 ± 34.94) compared with patients with EO-PD (73.64 ± 15.70; $p = 0.030$) and healthy controls (64.82 ± 24.60; $p < 0.001$) (Table II and Fig. 1). Also, LN and CN echogenicity indices were higher in patients with WD (109.10 ± 36.30 and 48.70 ± 21.00) compared with patients with EO-PD (62.60 ± 8.62, $p < 0.001$ and 39.52 ± 7.32; $p = 0.010$) and healthy controls (54.60 ± 14.06; $p < 0.001$ and 33.11 ± 8.78; $p < 0.001$),

Table I. Demography, clinical and transcranial sonographic findings

	WD patients	EO-PD patients	Control
Number of enrolled patients (males)	22 (11)	21 (10)	24 (8)
Age; mean ± SD (y)	43.8 ± 8.5	42.0 ± 4.5	37.6 ± 10.1
Duration of disease; mean ± SD (y)	17.2 ± 8.0	7.6 ± 4.8	NA
Duration of therapy; mean ± SD (y)	13.5 ± 7.2	3.6 ± 1.7	NA
UPDRS-III subscore; mean; median (interquartile range)	NA	21.3; 16.0 (12.0−32.0)	NA
UWDRS neurologic subscore; mean; median (interquartile range)	19.6; 13.5 (7.0−30.5)	NA	NA
L-DOPA equivalent; mean ± SD (mg)	NA	623.4 ± 453.2	NA
Number of patients on d-PEN/Zinc/combination treatment	7/8/4	NA	NA

d-PEN = d-penicillamine, EO-PD = early-onset Parkinson's disease, MRI = magnetic resonance imaging, SD = standard deviation, UPDRS-III = Unified Parkinson's Disease Rating Scale, Part III, UWDRS = Unified Wilson's Disease Rating Scale, WD = Wilson disease.

Table II. Transcranial sonography and magnetic resonance findings in WD, EO-PD and healthy controls

	WD patients (22 patients)	*p* value (WD versus EO-PD)	EO-PD patients (21 patients)	*p* value (EO-PD versus controls)	Controls (24 patients)	*p* value (WD versus controls)
Transcranial sonography						
Insula echogenicity index; mean ± SD	103.92 ± 34.94	0.030	73.64 ± 15.70	0.379	64.82 ± 24.60	<0.001
Hyperechogenic insula (>99th percentile in general population); *n* (%)	16 (72.7 %)	<0.001	1 (4.76 %)	0.984	1 (4.17 %)	<0.001
SN echogenicity index; mean ± SD	27.38 ± 5.60	<0.001	38.01 ± 8.65	<0.001	29.47 ± 5.27	0.475
Hyperechogenic SN (>90th percentile of general population); *n* (%)	3 (13.6 %)	<0.001	17 (81.0 %)	<0.001	2 (8.3 %)	0.741
LN echogenicity index; mean ± SD	109.10 ± 36.30	<0.001	62.60 ± 8.62	0.993	54.60 ± 14.06	<0.001
Hyperechogenic LN (>99th percentile in general population); *n* (%)	17 (77.3 %)	<0.001	0 (0 %)	1.000	0 (0 %)	<0.001
CN echogenicity index; mean ± SD	48.70 ± 21.00	0.010	39.52 ± 7.32	0.440	33.11 ± 8.78	<0.001
Hyperechogenic CN (>99th percentile in general population); *n* (%)	6 (27.3 %)	0.124	0 (0 %)	1.000	0 (0 %)	0.112
BR echogenicity index; mean ± SD	28.74 ± 4.92	0.531	31.67 ± 5.06	0.894	30.12 ± 5.12	0.697
Hypoechogenic BR (<fifth percentile in general population); *n* (%)	1 (4.5 %)	1.000	1 (4.8 %)	0.849	2 (8.3 %)	0.834
	Magnetic resonance					
Third ventricle width; mean ± SD	7.84 ± 2.70	0.016	3.98 ± 1.37	1.000	2.94 ± 0.54	0.002
Fourth ventricle width; mean ± SD	2.11 ± 0.52	0.563	2.00 ± 0.43	0.388	1.86 ± 0.23	0.168
Cortical atrophy - absent / mild / severe; *n* (%)	9(40.9)/7(31.8)/6(27.3)	0.667	7(33.3)/13(61.9)/1(4.8)	<0.001	24(100)/0(0)/0(0)	<0.001
Subcortical atrophy - absent / mild / severe; *n* (%)	6(27.2)/8(36.4)/8(36.4)	0.105	10(47.6)/8(38.1)/3(14.3)	<0.001	24(100)/0(0)/0(0)	<0.001
Cerebellar atrophy - absent / mild / severe; *n* (%)	4(18.2)/11(50.0)/7(31.8)	0.051	9(42.9)/9(42.9)/3(14.2)	<0.001	24(100)/0(0)/0(0)	<0.001

BR = brainstem raphe, CN = caudate nucleus, EO-PD = early-onset Parkinson's disease, LN = lentiform nucleus, SN = substantia nigra, WD = Wilson disease.

respectively. SN echogenicity index was higher in patients with EO-PD (38.01 ± 8.65) compared with patients with WD (27.38 ± 5.60; $p < 0.001$) and healthy controls (29.47 ± 5.27; $p < 0.001$) (Table II).

The width of the third ventricle was larger in patients with WD (7.84 ± 2.70 mm) compared with patients with EO-PD (3.98 ± 1.37 mm; $p = 0.016$) and healthy patients (2.94 ± 0.54 mm; $p = 0.002$) (Table II). Signs of cortical, subcortical and cerebellar atrophy on MR were significantly less frequent in healthy controls ($p < 0.001$ in all cases), but no significant differences were found between EO-PD and WD patients ($p = 0.667$, $p = 0.105$ and $p = 0.051$) (Table II). There were no correlations between echogenicity index of insula and age or NR echogenicity index, or between echogenicity of insula and width of third or fourth ventricle (Table III).

In patients with WD, the echogenicity index of insula was correlated with LN echogenicity index but not with age, disease duration, or symptom severity as assessed with the UWDRS. In patients with PD, there was no correlation among the echogenicity index of insula and any of the evaluated parameters (Table III).

DISCUSSION

The results of this study show that WD and EO-PD patients differ not only in terms of echogenicity of SN and LN but also in that of insula. Patients with WD exhibited increased echogenicity of both LN and insula compared with patients with EO-PD and healthy controls. Moreover, a strong positive correlation was

Table III. Correlation between echogenicity index of insula and selected parameters

		Echogenicity index of insula	
		Spearman correlation coefficient r	*p* value
All patients	Age	−0.01341	0.91423
	BR echogenicity index	−0.23556	0.05499
PD patients	Age	−0.13385	0.56296
	Disease duration	0.0595	0.79781
	UPDRS-III	−0.0883	0.74504
	SN echogenicity index	0.06623	0.77545
	Third ventricle width	−0.12602	0.58622
	Fourth ventricle width	0.28106	0.21714
	Cortical atrophy	−0.19645	0.39339
	Subcortical atrophy	0.18464	0.42300
WD patients	Age	−0.13834	0.53924
	Disease duration	−0.36091	0.09891
	UWDRS	0.27922	0.20824
	LN echogenicity index	0.74816	0.00006
	CN echogenicity index	0.2716	0.22145
	Third ventricle width	0.07064	0.75475
	Fourth ventricle width	0.12415	0.58200
	Cortical atrophy	0.11762	0.60216
	Subcortical atrophy	0.05641	0.8031

BR = brainstem raphe, CN = caudate nucleus, EO-PD = early-onset Parkinson's disease, LN = lentiform nucleus, SN = substantia nigra, UPDRS-III = the Unified Parkinson's Disease Rating Scale, Part III, UWDRS = the Unified Wilson's Disease Rating Scale, WD = Wilson's disease.

observed between the echogenicity of the two structures. These results confirm that insula echogenicity is a useful diagnostic marker for differentiating between WD and EO-PD.

The reason for the increased/decreased echogenicity of various brain structures in neurodegenerative diseases is not fully understood. Studies have shown that the accumulation of metals associated with neurodegeneration—for example, iron in PD (Berg et al. 1999; Behnke et al. 2009; Yu et al. 2018; Ghassaban et al. 2019), copper in WD (Walter et al. 2014), manganese in dystonia (Walter 2010), or calcification (Stenc Bradvica 2013)—may contribute to the increased echogenicity of brain parenchyma. On the contrary, decreased echogenicity of raphe nuclei may be attributable to neuronal loss in the central brainstem (Šilhán et al. 2015). In addition, other pathologic processes, such as focal brain atrophy (*e.g.,* medial temporal lobe in dementia) (Yilmaz et al. 2017) or pathologic intracranial processes (*e.g.,* tumor or hemorrhage) (Bogdahn et al. 1998; Školoudík 2017), can also lead to changes in brain parenchyma echogenicity.

The reason for increased insula echogenicity in patients with WD in our study is unclear; however, it is possible that copper or iron accumulation, structural changes associated with neuronal loss, gliosis and insular atrophy play a role. The strong correlation between insula and LN echogenicity suggests that the same pathologic process underlies the hyperechogenicity of the two structures.

A postmortem study showed that LN hyperechogenicity is correlated with putaminal copper but not iron concentration (Walter et al. 2014). Thus, copper accumulation and associated pathologic processes could lead to hyperechogenicity in both the LN and insula, although histopathologic analyses are needed to confirm this possibility.

Cortical and subcortical atrophy is another factor that could increase insula echogenicity. These were more frequently detected in patients with WD than in patients with EO-PD and healthy controls by MR. However, visually assessed cortical and subcortical atrophy were not correlated with insula echogenicity. Thus, the contribution of brain atrophy and accumulation of metals to insula echogenicity requires further quantitative magnetic resonance imaging study with volumetric analysis and a technique sensitive to metal deposits such as quantitative susceptibility mapping.

This study had several limitations. First, the number of patients was calculated only to evaluate differences in insula echogenicity between WD and PD patients and healthy controls; the influence of additional factors such as age, sex, disease stage, brain atrophy, or other brain pathologies on insula echogenicity remains to be determined. Second, the sensitivity and specificity of insula hyperechogenicity in diagnosing WD and differentiating between WD and EO-PD must be assessed using a larger number of treatment-naïve patients. Third, all TCS examinations were performed by only one highly experienced sonographer. Thus, the inter-investigator variability was not able to be evaluated. Moreover, the sonographer was not blinded to patients' movement disorder symptoms. Fourth, consistency and any variations along the planes within a group or across the groups were not tested. Last, serial TCS examinations should be performed to analyze the dynamics of insula echogenicity during the course of disease.

In conclusion, increased insula echogenicity in patients with WD compared with patients with PD and healthy controls was detected by TCS-MR fusion imaging. A strong positive correlation was observed between insula and LN echogenicity in patients with WD. Our findings indicate that insula echogenicity is a promising biomarker for WD.

Acknowledgments—The study was supported by Ministry of Health of the Czech Republic (grant number 15-25602 A), Charles University (Project PROGRES Q27/LF1) and IT4 Innovations Excellence in Science LQ1601.

Conflict of Interest disclosure—None of the authors report a conflict of interest with respect to financial or personal relationships with organizations that may have an influence on this work.

REFERENCES

Behnke S, Schroeder U, Dillmann U, Buchholz HG, Schreckenberger M, Fuss G, Reith W, Berg D, Krick CM. Hyperechogenicity of the substantia nigra in healthy controls is related to MRI changes and to neuronal loss as determined by F-Dopa PET. Neuroimage 2009;47:1237–1243.

Berg D, Godau J, Walter U. Transcranial sonography in movement disorders. Lancet Neurol 2008;7:1044–1055.

Berg D, Grote C, Rausch WD, Mäurer M, Wesemann W, Riederer P, Becker G. Iron accumulation in the substantia nigra in rats visualized by ultrasound. Ultrasound Med Biol 1999;25:901–904.

Blahuta J, Soukup T, Čermák P. Image processing of medical diagnostic neurosonographical images in MATLAB. recent researches in computer science. Proceedings of the 15th World Scientific and Engineering Academy and Society Circuits, Systems, Communications, and Computers Multiconference. : World Scientific and Engineering Academy and Society; 2011. p. 85–90.

Blahuta J, Soukup T, Jelínková M, Bártová P, Čermák P, Herzig R, Školoudík D. A new program for highly reproducible automatic evaluation of the substantia nigra from transcranial sonographic images. Biomed Pap Med Fac Univ Palacky Olomouc Czech Repub 2014;158:621–627.

Bogdahn U, Becker G, Schlachetzki F. Echoenhancers and transcranial color duplex sonography. 1st ed. Berlin: Blackwell Science Inc; 1998.

Forzoni L, D'Onofrio S, De Beni S, Laganà MM, Školoudík D, Baselli G, Nascente ISM. Virtual navigator registration procedure for transcranial application. In: Hellmich C, Hamza MH, Simsik D, (eds). Proceedings of the IASTED International Conference Biomedical Engineering (BioMed 2012). Innsbruck, Austria. : International Association of Science and Technology for Development (IASTED); 2012. p. 496–503.

Ghassaban K, He N, Sethi SK, Huang P, Chen S, Yan F, Haacke EM. Regional high iron in substantia nigra differentiates Parkinson's disease patients from healthy controls. Front Aging Neurosci 2019;11:106.

Laganà MM, Forzoni L, Viotti S, De Beni S, Baselli G, Cecconi P. Assessment of the cerebral venous system from the transcondylar ultrasound window using Virtual Navigator technology and MRI. In: Proceedings of 33rd Annual International Conference of the IEEE EMBS. Piscataway, NJ. : IEEE; 2011. p. 579–582.

Laganà MM, Preti MG, Forzoni L, D'Onofrio S, De Beni S, Barberio A, Cecconi P, Baselli G. Transcranial ultrasound and magnetic resonance image fusion with Virtual Navigator. IEEE T Multimedia 2013;15:1039–1048.

Mašková J, Školoudík D, Burgetová A, Fiala O, Brůha R, Záhoráková D, Serranová T, Slovák M, Ulmanová O, Růžička E, Dušek P. Comparison of transcranial sonography-magnetic resonance fusion imaging in Wilson's and early-onset Parkinson's diseases. Parkinsonism Relat Disord 2016;28:87–93.

Mijajlovic MD, Tsivgoulis G, Sternic N. Transcranial brain parenchymal sonography in neurodegenerative and psychiatric diseases. J Ultrasound Med 2014;33:2061–2068.

Šilhán P, Jelínková M, Walter U, Pavlov Praško J, Herzig R, Langová K, Školoudík D. Transcranial sonography of brainstem structures in panic disorder. Psychiatry Res 2015;234:137–143.

Školoudík D. Using transcranial sonography to display intracranial structures in the B-mode. Cesk Slov Neurol N 2017;80/113:8–23.

Školoudík D, Bártová P, Mašková J, Dušek P, Blahuta J, Langová K, Walter U, Herzig R. Transcranial sonography of the insula: Digitized image analysis of fusion images with magnetic resonance. Ultraschall Med 2016;37:604–608.

Školoudík D, Jelínková M, Blahuta J, Cermák P, Soukup T, Bártová P, Langová K, Herzig R. Transcranial sonography of the substantia nigra: Digital image analysis. AJNR Am J Neuroradiol 2014;35:2273–2278.

Školoudík D, Walter U. Method and validity of transcranial sonography in movement disorders. Int Rev Neurobiol 2010;90:7–34.

Stenc Bradvica I, Jančuljak D, Butković-Soldo S, Mihaljević I, Vladetić M, Bradvica M. Clinical manifestation and neuroimaging methods in diagnosing basal ganglia calcifications. Med Glas (Zenica) 2013;10:154–157.

Walter U. Transcranial sonography in brain disorders with trace metal accumulation. Int Rev Neurobiol 2010;90:166–178.

Walter U, Behnke S, Eyding J, Niehaus L, Postert T, Seidel G, Berg D. Transcranial brain parenchyma sonography in movement disorders: State of the art. Ultrasound Med Biol 2007;33:15–25.

Walter U, Školoudík D. Transcranial sonography of brain parenchyma in movement disorders: Quality standards, diagnostic applications and novel technologies. Ultraschall Med 2014;35:322–331.

Walter U, Skowrońska M, Litwin T, Szpak GM, Jabłonka-Salach K, Skoloudík D, Bulska E, Członkowska A. Lenticular nucleus hyperechogenicity in Wilson's disease reflects local copper, but not iron accumulation. J Neural Transm 2014;121:1273–1279.

Yilmaz R, Pilotto A, Roeben B, Preische O, Suenkel U, Heinzel S, Metzger FG, Laske C, Maetzler W, Berg D. Structural ultrasound of the medial temporal lobe in Alzheimer's disease. Ultraschall Med 2017;38:294–300.

Yu SY, Cao CJ, Zuo LJ, Chen ZJ, Lian TH, Wang F, Hu Y, Piao YS, Li LX, Guo P, Liu L, Yu QJ, Wang RD, Chan P, Chen SD, Wang XM, Zhang W. Clinical features and dysfunctions of iron metabolism in Parkinson disease patients with hyper echogenicity in substantia nigra: A cross-sectional study. BMC Neurol 2018;18:9.

Journal Pre-proof

Comparative Study of the Substantia Nigra Echogenicity and ^{123}i-Ioflupane Spect In Patients With Synucleinopathies With And Without Rem Sleep Behavior Disorder

J. Mašková, D. Školoudík, P. Štofaniková, V. Ibarburu, D. Kemlink, D. Zogala, J. Trnka, R. Krupička, K. Šonka, E. Růžička, P. Dušek

PII: S1389-9457(20)30085-X

DOI: https://doi.org/10.1016/j.sleep.2020.02.012 Reference: SLEEP 4331

To appear in: *Sleep Medicine*

Received Date: 6 November 2019

Revised Date: 16 January 2020

Accepted Date: 14 February 2020

Please cite this article as: Mašková J, Školoudík D, Štofaniková P, Ibarburu V, Kemlink D, Zogala D, Trnka J, Krupička R, Šonka K, Růžička E, Dušek P, Comparative Study of the Substantia Nigra Echogenicity and ^{123}i-Ioflupane Spect In Patients With Synucleinopathies With And Without Rem Sleep Behavior Disorder, *Sleep Medicine*, https://doi.org/10.1016/j.sleep.2020.02.012.

COMPARATIVE STUDY OF THE SUBSTANTIA NIGRA ECHOGENICITY AND ^{123}IIOFLUPANE SPECT IN PATIENTS WITH SYNUCLEINOPATHIES WITH AND WITHOUT REM SLEEP BEHAVIOR DISORDER

Mašková J.[1], Školoudík D [1,2], Štofaniková P.[1], Ibarburu V.[1], Kemlink D.[1], Zogala D.[3], Trnka J.[3], Krupička R.[4], Šonka K.[1], Růžička E.[1], Dušek P.[1,5]

1 Department of Neurology and Center of Clinical Neuroscience, First Faculty of Medicine, Charles University and General University Hospital Prague, Czech Republic

2 Department of Neurology, University Hospital Ostrava, Ostrava, Czech Republic

3 Institute of Nuclear Medicine, First Faculty of Medicine, Charles University and General University Hospital Prague, Czech Republic

4 Department of Biomedical Informatics, Czech Technical University in Prague, Faculty of Biomedical Engineering

5 Department of Radiology, First Faculty of Medicine, Charles University and General University Hospital Prague, Czech Republic

*Corresponding author:

Jana Mašková

Department of Neurology and Center of Clinical Neuroscience

Charles University

First Faculty of Medicine Charles University and General University Hospital Prague

Kateřinská 30, 120 00 Praha 2

Czech Republic

Tel: +420 22496 5527

Email: jana.maskova@vfn.cz

Study funding: Czech Science Foundation, grant nr. GACR 16-07879S

Abstract

Objectives: Hyperechogenicity of the substantia nigra (SN) and abnormal dopamine transporter-singlephoton emission computed tomography (DAT-SPECT) are biomarkers commonly used in the assessment of prodromal synucleinopathy. Our goal was: 1) to compare echogenicity of SN in idiopathic REM behavior disorder (iRBD), PD without RBD (PD-noRBD), PD with RBD (PD+RBD), and control subjects, and 2) to examine association between SN degeneration assessed by DATSPECT and SN echogenicity.

Patients/Methods: Sixty-one subjects with confirmed iRBD were examined using Movement Disorders Society-unified PD rating scale (MDS-UPDRS), TCS (transcranial sonography) and DATSPECT. The results were compared with 44 patients with PD (25% PD+RBD) and with 120 agematched healthy subjects.

Results and conclusion: The abnormal SN area was found in 75.5% PD, 23% iRBD and 7.3% controls. Median SN echogenicity area in PD (0.27 ± 0.22 cm^2) was higher compared to iRBD (0.07 ± 0.07 cm^2; $p<0.0001$) and controls (0.05 ± 0.03 cm^2; $p<0.0001$). SN echogenicity in PD+RBD was not significantly different from PD-noRBD (0.30 vs. 0.22, $p=0.15$).

Abnormal DAT-SPECT was found in 16 iRBD (25.4%) and 44 PD subjects (100%). No correlation between the larger SN area and corresponding putaminal binding index was found in iRBD ($r=-0.13$, $p=0.29$), nor in PD ($r=-0.19$, $p=0.22$).

The results of our study showed that: 1) SN echogenicity area in iRBD was higher compared to controls, but the hyperechogenicity was present only in a minority of iRBD; 2) SN echogenicity and DAT-SPECT binding index did not correlate in either group; and 3) SN echogenicity does not differ between PD with/without RBD.

Keywords: transcranial sonography, idiopathic rapid-eye-movement sleep behavior disorder, Parkinson's disease, dopamine transporter imaging, neuroimaging, substantia nigra hyperechogenicity

1. Introduction

Idiopathic rapid eye movement behavior disease (iRBD) is a disorder manifesting with typical dream-enacting behaviors and lack of atonia during REM sleep; it is recognized as prodromal phase of synucleinopathies[1-3] such as Parkinson's disease (PD), dementia with Lewy bodies (DLB)[4, 5], or multiple system atrophy (MSA). In contrast with previous works declaring average risk of conversion to manifest neurodegenerative phenotype between 38-68%[6-8], the recently published longitudinal studies revealed significant correlation between duration of follow-up and conversion rate[9] which exceeds 90% within 14 years since the first iRBD symptoms[10-12]. Additionally, in subjects presenting with other risk factors such as cognitive deficit, olfactory dysfunction, or abnormal findings in dopamine transporter-single-photon emission computed tomography imaging (DAT-SPECT), the phenoconversion rate is much higher[13].

DAT imaging is the gold standard for evaluating SN dopaminergic neuronal loss in prodromal and manifest synucleinopathies[14]. Gradual decrease in DAT binding observed in physiological aging (approximately 6-7% per decade) is accelerated in PD patients reaching 6-13% annual loss[14, 15]. Decrease below 65% of age-expected binding ratio was confirmed as a risk factor for the development of PD in elderly population[13]. The loss of DAT binding necessary for the clinical manifestation of parkinsonism is not exactly determined and the estimated threshold ranges from 50% to 80%[14, 16, 17]. Reduced striatal DAT binding in PD was associated with motor severity, mostly with bradykinesia and rigidity[18].

DAT imaging in iRBD is a useful marker for determination of short-term risk of conversion to manifest synucleinopathy[6]. However, it has been shown that a combination with other markers is required to achieve satisfactory predictive performance of the test towards conversion, e.g. inclusion of SN hyperechogenicity, which increases the sensitivity for conversion risk over 2.5 years to 100%[6]. Transcranial sonography (TCS) has been established as a specific and sensitive diagnostic tool for distinguishing PD patients from healthy subjects, achieving high specificity (83-87%) and sensitivity (93-100%)[19, 20]. Large SN hyperechogenic area, which is typically found in PD patients, is also consistently described in about 10% of the healthy population[21-23]. The presence of TCS SN hyperechogenicity is not associated with sex, or duration of clinical symptoms in PD and other synucleuinopathies[7, 24-30]. The previously reported age-independence of SN echogenicity changes [31-33] has been, however, re-evaluated and questioned in recent studies[34, 35].

The SN hyperechogenicity has been observed in iRBD subjects, although with a lower prevalence compared to PD[7, 26, 36, 37]. However, the results of previous studies evaluating TCS changes in iRBD are not entirely consistent: 1) reported average SN echogenicity area showed a wide range of values (0,16-

0,28 cm^2 in iRBD and 0,06-0,176 cm^2 in healthy subjects) and 2) the percentage of abnormal TCS findings varies in both groups (34-63% iRBD and 10-29% controls) [7, 36, 38-42].

Interestingly, iRBD patients do not reach the same extent of SN echogenicity area as is seen in PD, even after phenoconversion; this observation triggered birth of the theory postulating different mechanism of SN degeneration in PD with and without RBD[37]. Clinically, RBD is a marker of "diffuse malignant subtype" of synucleinopathies associated with a higher incidence of dementia, gait disturbance, and orthostasis[43, 44]. PD patients with RBD tend to have more severe SN dopaminergic loss on DAT-SPECT[45], however, it is not clear whether they also possess specific TCS signature.

Although both, TCS and DAT-SPECT, depict degeneration of SN, their longitudinal dynamics vary considerably. While the loss of dopaminergic neurons assessed by DAT-SPECT is progressive in time, the sonography studies have not shown dependence on the duration of the disease and the SN echogenicity changes in PD remain stationary over time[46]. Most of published studies documented no association between decreased striatal DAT uptake and SN hyperechogenicity in PD patients[18, 47], thus, they are considered as independent and complementary markers of SN damage[18, 38, 48].

Motivated by the knowledge gap regarding association between RBD status and TCS findings in synucleinopathies, the aims of our study were 1) to compare echogenicity of SN in control subjects, iRBD, PD without RBD (PD-noRBD), and PD with RBD (PD+RBD); 2) to examine association between SN degeneration assessed by DAT-SPECT and SN echogenicity; and 3) investigate association between SN echogenicity area and clinical severity of motor symptoms.

2. METHODS

2.1. Patients

Sixty-one subjects with iRBD (57M/4F, mean age 66.4±8.1) diagnosed according to the American Academy of Sleep Medicine ICSD-3 (International Classification of Sleep Disorders, 3rd ed, Darien, IL 2014) were included. For inclusion, all patients had to be without overt parkinsonism, dementia, factors indicative of secondary RBD such as narcolepsy, drug-induced RBD (i.e. RBD originating shortly after initiation of antidepressants), or focal brainstem lesions on MRI.

Forty-four treatment-naïve PD patients newly diagnosed in accordance with the MDS clinical diagnostic criteria[49, 50] (31M/13F, mean age 56.3±12.4 years) were included. All iRBD and PD patients were examined by a single-night polysomnography, the Movement Disorders Society-sponsored revision of the Unified PD Rating Scale (MDS-UPDRS)[51], TCS and DAT-SPECT. The PD group was divided into subroups without (PD-noRBD) and with (PD+RBD) RBD according to the results of the polysomnographic examination using identical criteria as in the iRBD group. Clinical and MDSUPDRS examination was performed by an experienced movement disorders specialist (PD, ER, VI).

The control group for TSC examination consisted of 120 healthy subjects (76M/44F, mean age 55.5±12.2 years) without history of neurological or psychiatric disorders. In all groups, only subjects with bilaterally permeable temporal bone window were included. All subjects signed informed consent and the study was approved by the Ethical Committee of General University Hospital in Prague.

2.2. Transcranial sonography (TCS)

In our study we used a commercial ultrasound device (Toshiba, Aplio 300) with a 2.5MHz phased array transducer. The ultrasound examination was performed through the right and left preauricular temporal bone windows with the commonly used parameters (penetration depth 16 cm, dynamic range 50 dB). The butterfly-shaped mesencephalic brainstem and the region of SN in mesencephalic section (Fig.1 A,B) were evaluated from the transverse plane. For accurate comparison, all TCS examinations were performed with the same settings without gain adjustment.

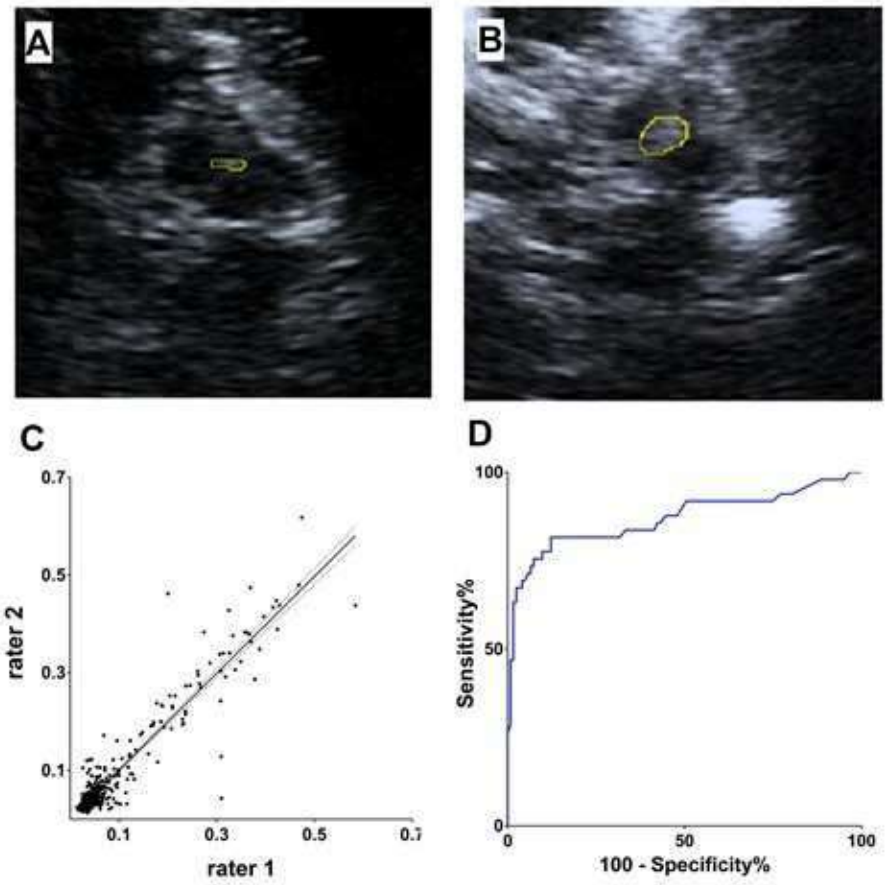

Figure 1 (double column fitting image) – TCS evaluation, hyperechogenic SN in hypoechogenic butterfly-like shape mesencephalon: Illustrative image of A) normal TCS (typical for healthy controls) and B) increased SN echogenicity (typical for PD); C) dot graph comparing SN area (cm^2) evaluations

from both raters; D) specificity and sensitivity in distinguishing PD and control group using the cut off value 0.126 cm^2

TCS examination was performed by a single experienced sonographer (JM), who was blinded to the clinical symptoms and patient history. The acquired mesencephalic sonographic images were converted to DICOM format and evaluated using ImageJ (NIH, MD, USA) by two independent raters (JM, PS) blinded to the diagnosis. The hyperechogenicity area was encircled manually in both sides. The intraclass correlation coefficient between raters confirmed high reliability of the assessment (r^2=0.87; p< 0.001; Fig.1C). The larger SN area from both sides was used for further analysis. As optimal cut off values may vary significantly between different sonographic devices and settings, we performed ROC analysis of SN area in a healthy cohort and PD group[52]. Using the optimal cut off value 0.126 cm^2 TCS reached 75.5% sensitivity and 92.7% specificity (p<0.0001) in distinguishing PD and control groups (Fig.1D).

The proportion of insufficiently permeable temporal bone windows on both sides in originally examined subjects was 24% in iRBD (n=19), 25% in PD (n=15), which is slightly higher compared to the usual published 5-20% range[7, 14, 38, 41, 53], but only 3,3% in healthy controls (n=23); these subjects are not included in the tables or analyses.

2.3. DAT SPECT

DAT-SPECT analysis was largely analogous to that used in a previous RBD study[54]. The examination was performed using the [123I]-2-b-carbomethoxy-3b-(4-iodophenyl)-N-(3-fluoropropyl) nortropane ([123I]FP-CIT, DaTscan®, GE Healthcare) tracer; approximately 185 MBq [123I]FP-CIT was injected intravenously. Scans were acquired 3 hours after tracer injection on a dual-head camera system (Infinia, GE Healthcare). The acquisition parameters were as follows: rotational radius 13-15 cm, image matrix 128×128, angular sampling with 120 projections at 3° interval and 40 seconds per view, zoom 1.3, energy window 159±10 % keV. Reconstruction of the raw SPECT projection data was performed using the ordered subset expectation maximization (OSEM) algorithm with 8 iterations and 10 subsets including Chang attenuation correction (μ = 0.11 cm−1) and 3D Butterworth postfiltering with FWHM = 8 mm. Automated semi-quantitative analysis was performed using the BasGan V2 software (https://www.aimn.it/site/page/gds/gds-5) and specific binding ratios (SBR) in the caudate nucleus and putamen in each hemisphere were calculated relative to a occipital reference region. Consequently, linear regression of age and caudate/ putamen SBR values in 97 healthy subjects included in the BasGan V2 software and 32 internal controls previously examined in the General University Hospital in Prague was calculated and 95%, one-sided prediction intervals was constructed. According to the putaminal

SBR from the hemisphere with lower tracer binding, DATSPECT scans with SBR < 95% prediction interval were classified as abnormal.

2.4. STATISTICS

Distributions of values of continuous variables were tested using the D'Agostino & Pearson normality test. Groupwise comparisons were done using either Student t-test, Mann-Whitney U test, KruskalWallis, one-way ANOVA or univariate general linear model with age and sex as covariates; post-hoc tests were corrected for multiple comparisons using the method of honestly significant difference test (HSD) as appropriate. Contingency analyses were performed using Pearson Chi-square or Fischer's exact test. Pearson correlation coefficient or partial correlation coefficient controlling for age and sex were used for testing of associations between variables. Statistica software version 12 (StatSoft) and Graphpad Prism version 6.07 (Graphpad software, San Diego, CA, USA) were used for statistical analysis.

3. RESULTS

3.1. Clinical assessment

Demographical data are shown in Tab.1. The iRBD group was slightly older ($p<0.001$) and with higher male/female ratio ($p<0.003$) compared to the PD and control group. The mean MDS-UPDRS III subscore in PD group was significantly higher compared to the iRBD group ($p <0.0001$).

Table 1 – Demographic data

	PD group	**iRBD group**	**Control group**	**p-value**
Number of patients (females); n	44 (13)	61 (4)	120 (44)	-
Age; mean ± SD (years)	56.3 ± 12.4	66.4 ± 8.1	55.5 ± 12.2	< 0.001*
Duration of subjective symptoms; mean ± SD (years) ⁑	2.3 ± 1.6	8.1 ± 9.0	N.A.	-
Interval between RBD diagnosis and TCS; mean ± SD (years)	-	0.69 ± 0.99	-	-
SN area; median ± IQR; mean ± SD× (cm^2)	0.27 ± 0.22; (0.23 ± 0.13)	0.07 ± 0.07; (0.11 ± 0.11)	0.05 ± 0.03; (0.06 ± 0.05)	< 0.003**

MDS-UPDRS-III subscore; mean ± SD	28.5 ± 13	6.4 ± 6.0	N.D.	< 0.0001

* One-way ANOVA, HSD post-hoc significant for iRBD vs controls and PD vs iRBD

** One-way ANOVA, HSD post-hoc test significant for PD vs. controls (p<0.0001); PD vs. iRBD (p<0.0001); and iRBD vs. controls (p<0.003)

× For comparison with previous studies, mean values are reported in brackets

⁑ Duration of motor symptoms in PD and dream-enactment behavior in iRBD

PD – Parkinson´s disease; iRBD – idiopathic REM behavior disorder; SD – standard deviation; SN – substantia nigra; IQR – interquartile range; MDS-UPDRS-III – Movement Disorder Society, Unified Parkinson´s Disease Rating Scale, motor examination

3.2. TCS findings

The abnormal SN area (>0.126 cm^2) was found in 75.5% PD, 23% iRBD and 7.3% controls; contingency analysis confirmed significantly higher proportion of abnormal SN area in iRBD patients compared to controls (OR 4.22 [95% confidence interval 1.75 – 10.22], p = 0.0007).

Quantitative analysis showed that SN area in PD was higher compared to iRBD (p<0.0001) and controls (p<0.0001); SN area was also higher in iRBD compared to controls (p<0.003, Tab.1). Sensitivity analysis comparing only iRBD patients and subgroup of age-matched controls confirmed significantly higher SN area in the iRBD group compared to controls (p<0.0001).

In order to examine whether the presence of RBD influences the SN area in the PD group, patients with and without RBD were compared. RBD was present in 11 (25%) PD patients (PD+RBD) and their SN echogenicity area was not significantly different compared to PD-noRBD (p=0.15, Tab.2).

Table 2 – SN echogenic area and DAT-SPECT specific binding ratios in iRBD and PD subgroups

	iRBD	**PD without RBD (PD-noRBD)**	**PD with RBD (PD+RBD)**	**p-value**
Number of patients (females)	61 (4)	33 (12)	11 (1)	<0.0005*
SN area (cm2), median ± IQR (higher from both hemisphere)	0.07 ± 0.08	0.30 ± 0.14	0.22 ± 0.02	<0.001**
Putaminal SBR (worse hemisphere)	2.9 ± 0.7	1.6 ± 0.3	1.2 ± 0.3	<0.0001***

Caudate SBR (worse hemisphere)	3.8 ± 0.8	3.3 ± 0.6	2.6 ± 0.7	<0.0004****

* Two-sided Fisher´s test for male/female ratio significant for iRBD vs PD-noRBD

** One-way ANOVA, HSD post-hoc test significant for iRBD vs PD-noRBD (p<0.002); and RBD vs. PD+RBD (p<0.001)

*** One-way ANOVA, HSD post-hoc test significant for iRBD vs PD-noRBD (p<0.0001); and RBD vs PD+RBD (p<0.0001)

**** One-way ANOVA, HSD post-hoc test significant for iRBD vs PD+RBD; RBD vs PD-noRBD; PD+RBD vs PD-noRBD (p<0.0004)

PD – Parkinson´s disease; RBD – REM behavior disorder; SN – substantia nigra; IQR – interquartile range; SBR – striatal binding ratio

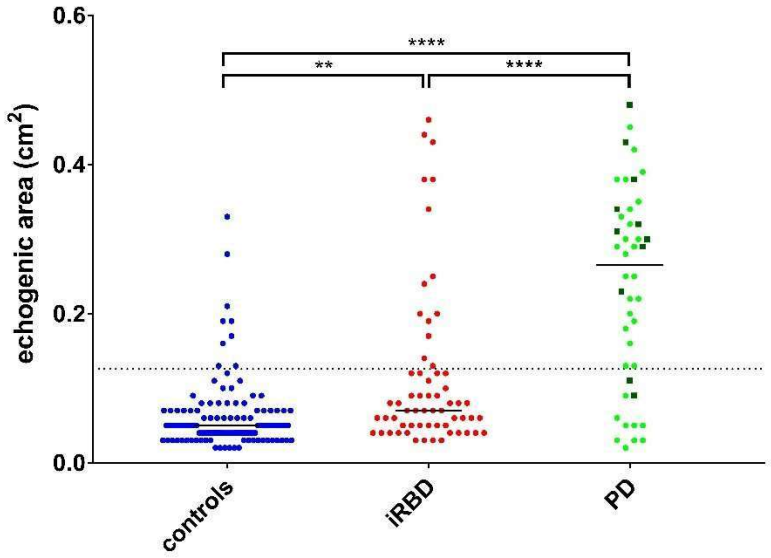

Figure 2 (single column fitting image) – Dot graphs comparing SN echogenic area in study groups (blue: controls, red: RBD, dark green rectangles: PD+RBD, light green circles: PD-noRBD)

3.3. DAT-SPECT findings

Abnormally decreased putaminal SBR was found in 16 (25.4%) iRBD and 44 (100%) PD patients. Corrected for age and sex, putaminal SBR from the worse hemisphere was significantly higher in the iRBD group, compared to the PD-noRBD group, and PD+RBD group (<0.0001). Caudate SBR from the worse hemisphere was also higher in iRBD compared to both PD-noRBD (p<0.0004) and PD+RBD (p<0.0004) subgroups; additionally, caudate SBR was lower in PD+RBD compared to PDnoRBD group (p<0.0004), see Tab.2).

3.4. Correlation between TCS, DAT-SPECT and clinical parameters

First, the larger SN area from bilateral TCS examination was used for the analysis and was compared with ipsilateral (corresponding) putaminal SBR. Contingency analysis comparing the concordance between DAT-SPECT and TCS findings showed that proportion of abnormal DAT-SPECT was not significantly different in iRBD patients with abnormal (35.7%) compared to normal (21.2%) TCS finding (p=0.28).

Quantitative comparison of patients with normal and abnormal TCS findings confirmed there were no differences in putaminal SBR, corrected for age and sex, corresponding to the SN with larger hyperechogenic area in both, iRBD (p=0.45) and PD group (p=0.80). Analysis of caudate SBR returned similar results (p=0.63 in iRBD and p=0.84 in PD group) (Tab.3). Partial correlation analysis corrected for age and sex showed no association between the larger SN area and putaminal SBR from the corresponding hemisphere in iRBD (r=-0.13, p=0.29), nor in PD group (r=-0.19, p=0.22), see Fig.3.

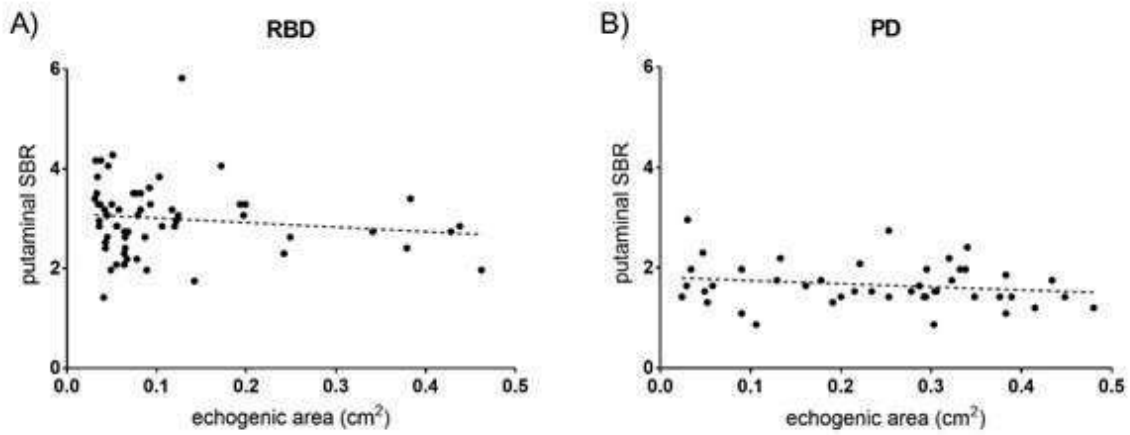

Figure 3 (double column fitting image) – Scatter graphs of correlation between putaminal SBR and SN area in A) iRBD and B) PD group.

Additionally, we did not find a difference in gender (p=0.71), nor in the mean age of symptoms onset between PD patients with normal (54.1 ± 15.2 years) and abnormal (54.2 ± 12.0 years) TCS findings. We also did not find correlation between the SN echogenicity area and age in neither group (r=0.17, p=0.18 in iRBD; r=0.11, p=0.49 in PD; r=0.10, p=0.28 in controls; Fig. 4).

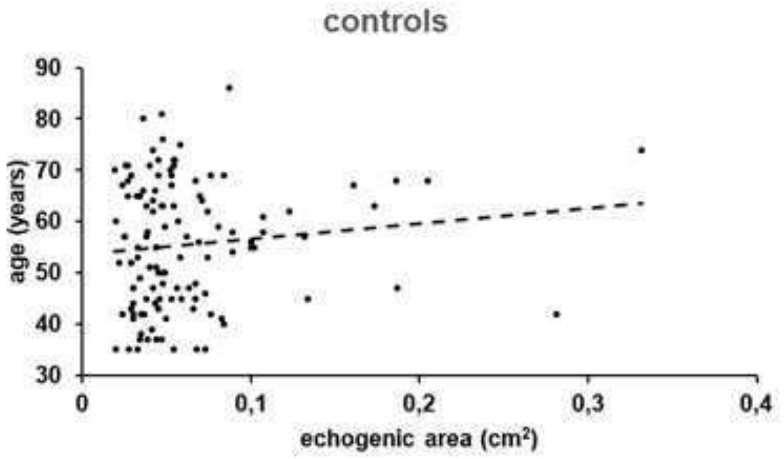

Figure 4 (single column fitting image) – Distribution of SN area according to age in healthy controls

Next, the influence of TCS and DAT-SPECT findings on motor function was examined; iRBD patients with normal findings on both (TCS and DAT-SPECT) examination methods had significantly lower MDS-UPDRS III score (4.9±3.9) compared to patients with abnormality in at least one examination method (8.8±6.9; p=0.03), see Tab.4. Additionally, partial correlation analysis corrected for age and sex showed that MDS-UPDRS-III score was associated with SN echogenicity area in iRBD group (r=0.27, p=0.045) and with putaminal SBR in PD group (r=-0.37, p=0.005).

Table 4 – Proportion of iRBD subjects with normal and abnormal TCS and DAT-SPECT findings

		Abnormal SN area	**Normal SN area**
Abnormal putaminal SBR	Number of subjects; n	5	10
	MDS-UPDRS III subscore; mean ± SD	6.4 ± 3.6	9.0 ± 9.0
Normal putaminal SBR	Number of subjects; n	9	37
	MDS-UPDRS III subscore; mean ± SD	9.9 ± 5.8	4.9 ± 3.9

SN – substantia nigra; SBR – striatal binding ratio; SD – standard deviation; MDS-UPDRS-III – Movement Disorder Society, Unified Parkinson´s Disease Rating Scale, motor examination

4. DISCUSSION

The results confirmed that: 1) the median SN echogenicity area in iRBD patients is slightly higher than that of controls, but values exceeding the cut off were present only in a minority of iRBD patients

and 2) TCS SN area and DAT-SPECT binding indexes are not correlated in either, iRBD or PD group. In addition, we found that: 3) SN area does not differ between PD+RBD and PD-noRBD and 4) motor function assessed by MDS-UPDRS III score was best preserved in iRBD patients with normal TCS and DAT-SPECT results.

The median values of SN area differed between the studied groups (PD>iRBD>healthy subjects), whereas the overall proportion of abnormal TCS finding was significantly higher in iRBD compared to healthy controls. The structural causes of the SN echogenicity changes are not well understood and may theoretically involve the role of iron deposits, glial activation or vascular changes[55-59]. The cut off value for SN area calculated for our data (0.126 cm^2) is smaller than the usually mentioned value 0.20 cm^2 (Tab.5). The higher cut off values in previously published studies could be influenced by several factors: a) using different image processing of ultrasound device providers and previously published cut offs instead of calculating own specific values (see Tab.5 listing cut offs used in previous studies), b) adjusting the gain parameters, which can lead to the overestimation of the SN area and c) different strategies of SN area encircling.

Importantly, our cut off is based on analysis of results from two independent raters with a high between-rater agreement and its sensitivity and specificity are comparable to previous studies[30, 53, 57, 59] (Fig.1 C,D). Unlike the previous publications, we used the median instead of the mean for SN area evaluation, because the distribution of values of SN area in healthy controls and iRBD subjects was abnormal.

Table 5 – Previously published TCS cut-off values in iRBD studies

First author + (publication year)	**Cut off value (cm^2)**	**iRBD SN area (cm^2)**	**PD SN area (cm^2)**	**Control group SN area (cm^2)**	**Number of iRBD patients (abnormal TCS in %)**	**Ultrasound device**
Iwanami et al (2010)[26]	0,20 (take over cut off)	0.20 ± 0.13	0.22 ± 0.11	0.06 ± 0.06	34 (41.2)	Logic 7, GE
Stockner et al (2009)[7]	0,20 (90th percentile)	0.20 ± 0.09	N.A.	0.14 ± 0.05	51 (37.3)	Logic 7, GE
Iranzo et al (2010)[38]	0,20 (90th percentile)	0.20 ±0.09	N.A.	0.14 ± 0.05	39 (36.0)	Logic 7, GE
Shin et al (2012)[39]	0,20 (take over cut off)	0.29 ± 0.47	0.72 ± 0.41	0.11 ± 0.17	12 (50.0)	Philips
Vilas et al (2015)[40]	0,20 (take over cut off)	0.24 ± 0.10	N.A.	0.176 ± 0.11	59 (62.7)	Phillips

Miyamoto et al (2013)[36]	0,18 (take over cut off)	N.A.	N.A.	N.A.	N.A.	N.A.
Iranzo et al (2014)[41]	0,20 (take over cut off)	0.20 ± 0.09	N.A.	N.A.	31 (32.3)	Logic 7, GE
Noyce et al. (2018)[42]	0,16 (take over cut off)	N.A.	N.A.	N.A.	N.A.	GE Healthcare

REM – rapid eye movement; SN – substantia nigra; iRBD - idiopathic REM behavior disorder

Moreover, all sonographic images were acquired using the same TCS settings. These factors likely contributed to lower SN area and higher number of excluded patients due to the poor temporal bone window quality.

Abnormal TCS findings were present only in 23% iRBD patients. Previously published studies referred a higher proportion of iRBD patients with abnormal SN echogenicity area (from 32.3% to 62.7%)[7, 26, 36, 38, 39, 41, 60]. The highest SN area was reported in study with a relatively low number of subjects (n=12) and short duration of symptoms (5.3 years)[39], which might lead to biased estimate. Aggregate results in all patients from the studies listed in Tab. 5 yields abnormal TCS findings in 44.2% iRBD subjects which is almost double the prevalence of pathological findings in this study. The main reason for the low percentage of TCS abnormalities is likely to be the use of other methodologies of SN area assessment. Especially we have used cut off value defined as optimal value for discrimination of PD and controls based on ROC analysis. Lowering the cut off value to 0.1 cm^2, which is the 90th percentile of SN area in the control cohort, yields abnormal TCS finding in 32.4% RBD patients. Thus, using commonly employed method for cut off value determination makes the estimate of abnormal TCS finding prevalence in our RBD cohort more comparable to previous findings. We also cannot exclude the influence of other factors such as device settings or different composition of our RBD cohort).

The results confirmed that SN echogenicity is not associated with reduced striatal DAT uptake in any of examined groups. Moreover, in some subjects, the hemisphere with abnormal DAT-SPECT and enlarged SN area differed, which further confirms that these neuroimaging abnormalities are unrelated. Our conclusion corresponds to results of previously published studies[18, 38, 48].

To our best knowledge, this is the first study comparing TCS findings in PD patients with and without RBD. Most of the previously published studies comparing PD with and without RBD focused mainly on the difference of clinical[44, 61] and DAT-SPECT findings. In our study, patients with prodromal (iRBD) and manifest (PD+RBD) synucleinopathy presenting with RBD differed in both, DAT-SPECT and TCS, results with significantly worse findings in PD+RBD. According to a prospective study by Iranzo et al,

presence of RBD may mark a distinctive synucleinopathy phenotype with different mechanisms of neurodegeneration[10]. Abnormal SN hyperechogenic area is present not only in PD with and without RBD, but also in DLB, a disorder with high frequency of RBD and bilateral TCS abnormities[5, 62].

Idiopathic RBD patients with normal TCS and normal DAT-SPECT have significantly lower motor deficit in the study suggesting that pathology in either type of examination has some functional consequence. It has been shown that pathology in both methods, TCS and DAT-SPECT, is a risk factor for early phenoconversion[38, 41]. However, the importance of normal SN echogenicity alone for RBD phenoconversion has also not yet been properly assessed. Based on our observations, we assume that normal SN area in synucleinopathies is not associated with RBD in general but appears to be common in patients with RBD preceding the development of parkinsonism with a longer time delay. Although a smaller SN area in PD was previously found to be associated with later onset of symptoms[63], we did not confirm this result. We speculate that hyperechogenic SN is more vulnerable to alpha-synuclein pathology and TCS abnormality could thus represent a risk factor for the appearance of motor symptoms with less severe degeneration of dopaminergic neurons. On the contrary, dopaminergic neurons in subjects with normal SN echogenic area may be less sensitive to the effect of alpha-synuclein pathology, which may first present by symptoms of damage of other nuclei before parkinsonism manifests. These theories will have to be verified by long-term observation of larger number of RBD subjects.

Association between abnormal TCS finding and worse MDS-UPDRS III score previously found in elderly population[64] was only partially confirmed in iRBD patients in our study. Besides mild correlation between MDS-UPDRS III and SN area, the difference in motor function between iRBD patients with normal and abnormal TCS finding became significant only when putaminal DATSPECT binding was taken into account. This finding is consistent with the assumption that SN hyperechogenicity alone does not significantly affect the severity of motor deficit, but with simultaneous neurodegenerative process becomes a fragile terrain for early nigrostriatal dysfunction.

The limitations of the study were the cross-sectional design, absence of DAT-SPECT examination and MDS-UPDRS III score in healthy subjects, and relatively small number of PD patients with RBD. Further limitation were slightly higher age and the predominance of males in the iRBD group. Importantly, several studies have shown no correlation between gender, age and SN echogenic area[41]43 indicating that slight age and gender imbalance have not significantly biased our results.

The results of our study confirmed different SN echogenicity changes in PD, iRBD and control group. According to the findings, iRBD patients have a relatively low prevalence of abnormal TCS findings,

while the SN echogenicity pattern in PD with RBD is comparable to PD without RBD. Thus, patients with long-term iRBD preceding phenoconversion likely represent a specific phenotype of synucleinopathy. Normal TCS and DAT-SPECT findings are associated with normal motor function in iRBD patients. Finally, we conclude that the SN hyperechogenicity reflects structural and DAT-SPECT functional changes in dopaminergic pathway. TCS and DAT-SPECT examinations are complementary but not substitutable.

Acknowledgements

This study was supported by Czech Science Foundation, grant nr. GACR 16-07879S

Conflict of interest

The authors declare that they have no conflict of interest.

References

1. Postuma RB, Gagnon JF, Montplaisir JY. REM Sleep Behavior Disorder and Prodromal Neurodegeneration - Where Are We Headed? Tremor Other Hyperkinet Mov (N Y) 2013;3.
2. Postuma RB. Prodromal Parkinson's disease--using REM sleep behavior disorder as a window. Parkinsonism Relat Disord 2014;20 Suppl 1:S1-4.
3. Hogl B, Stefani A, Videnovic A. Idiopathic REM sleep behaviour disorder and neurodegeneration - an update. Nature reviews Neurology 2018;14:40-55.
4. Walter U, Dressler D, Wolters A, Wittstock M, Greim B, Benecke R. Sonographic discrimination of dementia with Lewy bodies and Parkinson's disease with dementia. J Neurol 2006;253:448-454.
5. Favaretto S, Walter U, Baracchini C, et al. Accuracy of transcranial brain parenchyma sonography in the diagnosis of dementia with Lewy bodies. Eur J Neurol 2016;23:1322-1328.
6. Iranzo A, Molinuevo JL, Santamaria J, et al. Rapid-eye-movement sleep behaviour disorder as an early marker for a neurodegenerative disorder: a descriptive study. Lancet Neurol 2006;5:572-577.

7. Stockner H, Iranzo A, Seppi K, et al. Midbrain hyperechogenicity in idiopathic REM sleep behavior disorder. Mov Disord 2009;24:1906-1909.
8. Postuma RB, Montplaisir J. Transcranial ultrasound and olfaction in REM sleep behavior disorder: testing predictors of Parkinson's disease. Sleep Med 2010;11:339-340.
9. Galbiati A, Verga L, Giora E, Zucconi M, Ferini-Strambi L. The risk of neurodegeneration in REM sleep behavior disorder: A systematic review and meta-analysis of longitudinal studies. Sleep Med Rev 2018;43:3746.
10. Iranzo A, Fernandez-Arcos A, Tolosa E, et al. Neurodegenerative disorder risk in idiopathic REM sleep behavior disorder: study in 174 patients. PLoS One 2014;9:e89741.
11. Postuma RB. Prodromal Parkinson disease: do we miss the signs? Nat Rev Neurol 2019;15:437-438.
12. Postuma RB, Iranzo A, Hu M, et al. Risk and predictors of dementia and parkinsonism in idiopathic REM sleep behaviour disorder: a multicentre study. Brain 2019;142:744-759.
13. Jennings D, Siderowf A, Stern M, et al. Conversion to Parkinson Disease in the PARS Hyposmic and Dopamine Transporter-Deficit Prodromal Cohort. JAMA Neurol 2017;74:933-940.
14. Shih MC, Hoexter MQ, Andrade LA, Bressan RA. Parkinson's disease and dopamine transporter neuroimaging: a critical review. Sao Paulo Med J 2006;124:168-175.
15. van Dyck CH, Seibyl JP, Malison RT, et al. Age-related decline in striatal dopamine transporter binding with iodine-123-beta-CITSPECT. J Nucl Med 1995;36:1175-1181.
16. Isaias IU, Trujillo P, Summers P, et al. Neuromelanin Imaging and Dopaminergic Loss in Parkinson's Disease. Front Aging Neurosci 2016;8:196.
17. Fearnley JM, Lees AJ. Ageing and Parkinson's disease: substantia nigra regional selectivity. Brain 1991;114 (Pt 5):2283-2301.
18. Spiegel J, Hellwig D, Mollers MO, et al. Transcranial sonography and [123I]FP-CIT SPECT disclose complementary aspects of Parkinson's disease. Brain 2006;129:1188-1193.
19. Walter U, Behnke S, Eyding J, et al. Transcranial brain parenchyma sonography in movement disorders: state of the art. Ultrasound Med Biol 2007;33:15-25.
20. Berg D, Godau J, Walter U. Transcranial sonography in movement disorders. Lancet Neurol 2008;7:1044-1055.
21. Bouwmans AE, Vlaar AM, Srulijes K, Mess WH, Weber WE. Transcranial sonography for the discrimination of idiopathic Parkinson's disease from the atypical parkinsonian syndromes. Int Rev Neurobiol 2010;90:121-146.
22. Busse K, Heilmann R, Kleinschmidt S, et al. Value of combined midbrain sonography, olfactory and motor function assessment in the differential diagnosis of early Parkinson's disease. J Neurol Neurosurg Psychiatry 2012;83:441-447.
23. Kim JS, Oh YS, Kim YI, Koo JS, Yang DW, Lee KS. Transcranial sonography (TCS) in Parkinson's disease (PD) and essential tremor (ET) in relation with putative premotor symptoms of PD. Arch Gerontol Geriatr 2012;54:e436-439.
24. Pilotto A, Yilmaz R, Berg D. Developments in the role of transcranial sonography for the differential diagnosis of parkinsonism. Curr Neurol Neurosci Rep 2015;15:43.
25. Alonso-Canovas A, Lopez-Sendon JL, Buisan J, et al. Sonography for diagnosis of Parkinson diseasefrom theory to practice: a study on 300 participants. J Ultrasound Med 2014;33:2069-2074.
26. Iwanami M, Miyamoto T, Miyamoto M, Hirata K, Takada E. Relevance of substantia nigra hyperechogenicity and reduced odor identification in idiopathic REM sleep behavior disorder. Sleep medicine 2010;11:361-365.
27. Bartova P, Skoloudik D, Ressner P, Langova K, Herzig R, Kanovsky P. Correlation between substantia nigra features detected by sonography and Parkinson disease symptoms. J Ultrasound Med 2010;29:37-42.
28. Ambrosius W, Michalak S, Owecki M, Lukasik M, Florczak-Wyspianska J, Kozubski W. Substantia nigra hyperechogenicity in Polish patients with Parkinson's disease. Folia Morphol (Warsz) 2014;73:267-271.
29. Walter U, Dressler D, Wolters A, Wittstock M, Benecke R. Transcranial brain sonography findings in clinical subgroups of idiopathic Parkinson's disease. Mov Disord 2007;22:48-54.

30. Ressner P, Skoloudik D, Hlustik P, Kanovsky P. Hyperechogenicity of the substantia nigra in Parkinson's disease. J Neuroimaging 2007;17:164-167.
31. Berg D, Siefker C, Ruprecht-Dorfler P, Becker G. Relationship of substantia nigra echogenicity and motor function in elderly subjects. Neurology 2001;56:13-17.
32. Mehnert S, Reuter I, Schepp K, Maaser P, Stolz E, Kaps M. Transcranial sonography for diagnosis of Parkinson's disease. BMC Neurol 2010;10:9.
33. Walter U, Niehaus L, Probst T, Benecke R, Meyer BU, Dressler D. Brain parenchyma sonography discriminates Parkinson's disease and atypical parkinsonian syndromes. Neurology 2003;60:74-77.
34. Toomsoo T, Liepelt-Scarfone I, Berg D, et al. Effect of Age on Substantia Nigra Hyper-echogenicity in Parkinson's Disease Patients and Healthy Controls. Ultrasound Med Biol 2019;45:122-128.
35. Hagenah J, Konig IR, Sperner J, et al. Life-long increase of substantia nigra hyperechogenicity in transcranial sonography. Neuroimage 2010;51:28-32.
36. Miyamoto M, Miyamoto T. Neuroimaging of rapid eye movement sleep behavior disorder: transcranial ultrasound, single-photon emission computed tomography, and positron emission tomography scan data.
Sleep Med 2013;14:739-743.
37. Iranzo A, Santamaria J, Valldeoriola F, et al. Dopamine transporter imaging deficit predicts early transition to synucleinopathy in idiopathic rapid eye movement sleep behavior disorder. Ann Neurol 2017;82:419-428.
38. Iranzo A, Lomena F, Stockner H, et al. Decreased striatal dopamine transporter uptake and substantia nigra hyperechogenicity as risk markers of synucleinopathy in patients with idiopathic rapid-eye-movement sleep behaviour disorder: a prospective study [corrected]. Lancet Neurol 2010;9:1070-1077.
39. Shin HY, Joo EY, Kim ST, Dhong HJ, Cho JW. Comparison study of olfactory function and substantia nigra hyperechogenicity in idiopathic REM sleep behavior disorder, Parkinson's disease and normal control.
Neurol Sci 2013;34:935-940.
40. Vilas D, Iranzo A, Pont-Sunyer C, et al. Brainstem raphe and substantia nigra echogenicity in idiopathic REM sleep behavior disorder with comorbid depression. J Neurol 2015;262:1665-1672.
41. Iranzo A, Stockner H, Serradell M, et al. Five-year follow-up of substantia nigra echogenicity in idiopathic REM sleep behavior disorder. Mov Disord 2014;29:1774-1780.
42. Noyce AJ, Dickson J, Rees RN, et al. Dopamine reuptake transporter-single-photon emission computed tomography and transcranial sonography as imaging markers of prediagnostic Parkinson's disease. Mov Disord 2018;33:478-482.
43. Romenets SR, Gagnon JF, Latreille V, et al. Rapid eye movement sleep behavior disorder and subtypes of Parkinson's disease. Mov Disord 2012;27:996-1003.
44. Liu Y, Zhu XY, Zhang XJ, Kuo SH, Ondo WG, Wu YC. Clinical features of Parkinson's disease with and without rapid eye movement sleep behavior disorder. Transl Neurodegener 2017;6:35.
45. Bauckneht M, Chincarini A, De Carli F, et al. Presynaptic dopaminergic neuroimaging in REM sleep behavior disorder: A systematic review and meta-analysis. Sleep Med Rev 2018;41:266-274.
46. Berg D. Transcranial sonography in the early and differential diagnosis of Parkinson's disease. J Neural Transm Suppl 2006:249-254.
47. Dusek P, Roos PM, Litwin T, Schneider SA, Flaten TP, Aaseth J. The neurotoxicity of iron, copper and manganese in Parkinson's and Wilson's diseases. Journal of trace elements in medicine and biology : organ of the Society for Minerals and Trace Elements 2015;31:193-203.
48. Doepp F, Plotkin M, Siegel L, et al. Brain parenchyma sonography and 123I-FP-CIT SPECT in Parkinson's disease and essential tremor. Mov Disord 2008;23:405-410.
49. Postuma RB, Berg D, Stern M, et al. MDS clinical diagnostic criteria for Parkinson's disease. Mov Disord 2015;30:1591-1601.
50. Postuma RB, Poewe W, Litvan I, et al. Validation of the MDS clinical diagnostic criteria for Parkinson's disease. Mov Disord 2018;33:1601-1608.

51. Goetz CG, Tilley BC, Shaftman SR, et al. Movement Disorder Society-sponsored revision of the Unified Parkinson's Disease Rating Scale (MDS-UPDRS): scale presentation and clinimetric testing results. Mov Disord 2008;23:2129-2170.
52. Li DH, He YC, Liu J, Chen SD. Diagnostic Accuracy of Transcranial Sonography of the Substantia Nigra in Parkinson's disease: A Systematic Review and Meta-analysis. Sci Rep 2016;6:20863.
53. Fernandes Rde C, Rosso AL, Vincent MB, et al. Transcranial sonography as a diagnostic tool for Parkinson's disease: a pilot study in the city of Rio de Janeiro, Brazil. Arq Neuropsiquiatr 2011;69:892-895. 54. Dušek P, Ibarburu VLyL, Bezdicek O, et al. Relations of non-motor symptoms and dopamine transporter binding in REM sleep behavior disorder. Scientific Reports 2019;9:15463.
55. Ouchi Y, Yoshikawa E, Sekine Y, et al. Microglial activation and dopamine terminal loss in early Parkinson's disease. Ann Neurol 2005;57:168-175.
56. Berg D, Merz B, Reiners K, Naumann M, Becker G. Five-year follow-up study of hyperechogenicity of the substantia nigra in Parkinson's disease. Mov Disord 2005;20:383-385.
57. Berg D, Grote C, Rausch WD, et al. Iron accumulation in the substantia nigra in rats visualized by ultrasound. Ultrasound Med Biol 1999;25:901-904.
58. Berg D, Godau J, Riederer P, Gerlach M, Arzberger T. Microglia activation is related to substantia nigra echogenicity. J Neural Transm (Vienna) 2010;117:1287-1292.
59. Berg D, Roggendorf W, Schroder U, et al. Echogenicity of the substantia nigra: association with increased iron content and marker for susceptibility to nigrostriatal injury. Arch Neurol 2002;59:999-1005.
60. Unger MM, Moller JC, Stiasny-Kolster K, et al. Assessment of idiopathic rapid-eye-movement sleep behavior disorder by transcranial sonography, olfactory function test, and FP-CIT-SPECT. Mov Disord 2008;23:596-599.
61. Yan YY, Lei K, Li YY, Liu XF, Chang Y. The correlation between possible RBD and cognitive function in Parkinson's disease patients in China. Ann Clin Transl Neurol 2019;6:848-853.
62. Walter U, Dressler D, Wolters A, Probst T, Grossmann A, Benecke R. Sonographic discrimination of corticobasal degeneration vs progressive supranuclear palsy. Neurology 2004;63:504-509.
63. Berg D, Siefker C, Becker G. Echogenicity of the substantia nigra in Parkinson's disease and its relation to clinical findings. J Neurol 2001;248:684-689.
64. Berg D, Seppi K, Liepelt I, et al. Enlarged hyperechogenic substantia nigra is related to motor performance and olfaction in the elderly. Mov Disord 2010;25:1464-1469.

Table 3 – Clinical and imaging findings in PD and iRBD subgroups with normal and abnormal TCS

	iRBD/ normal TCS	**iRBD/ abnormal TCS**	**p-value**	**PD/ normal TCS**	**PD/ abnormal TCS**	**pvalue**
Number (females); n	47 (4)	14 (0)	0.56	11 (4)	33 (9)	0.71
Age; mean ± SD (years)	65.7± 8.4	68.5 ± 6.1	0.89	57.0 ± 13.9	56.0 ± 11.6	1.00
Duration of subjective symptoms; mean ± SD (years)	9.0 ± 9.5	4.8 ± 4.2	0.36	2.2 ± 6.4	2.2 ± 1.6	1.00
Corresponding putaminal SBR; mean ± SD	3.00 ± 0.63	3.02 ± 0.97	1.00	1.70 ± 0.58	1.65 ± 0.39	1.00
Corresponding caudate SBR; mean ± SD	3.76 ± 0.74	3.55 ± 0.49	0.63	3.15 ± 0.83	3.09 ± 0.60	0.84
MDS-UPDRS-III subscore; mean ± SD	5.6 ± 5.49	8.6 ± 5.05	0.84	32.3 ± 14.26	27.2 ± 12.2	0.59

iRBD – idiopathic REM behavior disorder; MDS-UPDRS-III – Movement Disorder Society, Unified Parkinson´s Disease Rating Scale, motor score; PD – Parkinson´s disease; SN – substantia nigra; SBR – specific binding ratio; SD – standard deviation, TCS – transcranial sonography

Highlights:

- Substantia nigra hyperechogenicity was found only in 23% of iRBD patients
- In PD patients, substantia nigra hyperechogenicity is not influenced by the presence of RBD
- Substantia nigra echogenicity and decreased dopamine transporter binding are unrelated markers

CRediT Author Statement

Mašková Jana: Conceptualization, Validation, Formal analysis, Investigation, Writing - Original Draft, Writing - Review & Editing, Visualization

Školoudík David: Methodology, Software, Writing - Review & Editing

Štofaniková Petra: Validation, Formal analysis

Ibarburu Veronika: Investigation, Validation, Formal analysis,

Kemlink David: Validation, Formal analysis, Writing - Review & Editing

Zogala David: Investigation, Formal analysis, Resources

Trnka Jiří: Investigation, Methodology, Formal analysis

Krupička Radim: Methodology, Formal analysis

Šonka Karel: Resources, Writing - Review & Editing, Supervision, Funding acquisition

Růžička Evžen: Resources, Writing - Review & Editing, Supervision, Funding acquisition

Dušek Petr: Conceptualization, Methodology, Validation, Formal analysis, Investigation, Writing - Original Draft, Writing - Review & Editing, Visualization, Supervision, Funding acquisition